

2

---

# BISPECTRA

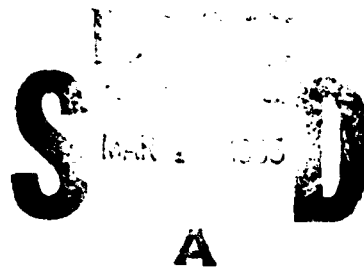
---

Henry Abarbanel  
Russ Davis  
Gordon J. MacDonald  
Walter Munk

January 1985

JSR-83-204

Approved for public release; distribution unlimited.



JASON  
The MITRE Corporation  
1820 Dolley Madison Boulevard  
McLean, Virginia 22102

This document has been approved  
for public release and sale; its  
distribution is unlimited.



TABLE OF CONTENTS

	<u>Page</u>
LIST OF ILLUSTRATIONS .....	iv
INTRODUCTION .....	1
1.0 A PRIMER ON HIGHER-ORDER OF POLYSPECTRA.....	6
1.1 Linear and Non-Linear Models.....	7
1.2 Polyspectra .....	13
1.3 Polyspectra for Gaussian Processes.....	17
1.4 Cross Polyspectrum .....	18
1.5 Meaning of a Finite Bispectrum.....	24
2.0 BISPECTRAL DETECTION.....	27
2.1 Introduction .....	27
2.2 The Three Detectors.....	29
2.3 Simplified Performance Measures.....	32
2.4 Comparison .....	37
2.5 Conclusion .....	39
3.0 BISPECTRAL EXPERIMENTS.....	42
3.1 Introduction .....	42
3.2 Power Spectrum.....	43
3.3 Bispectra .....	51
3.4 Discussion .....	61
4.0 BISPECTRAL LOCALIZATION.....	63
4.1 Introduction .....	63
4.2 The Bi-Phase .....	64
4.3 The Simplest Case.....	65
4.4 Interpretation of Sources.....	68
4.5 Other Frequency Ratios.....	69
BIBLIOGRAPHY ON THE BISPECTRUM.....	70
DISTRIBUTION LIST .....	D-1

Accession For	
NTIS GRA&I <input checked="" type="checkbox"/>	
DTIC TAB <input type="checkbox"/>	
Unannounced <input type="checkbox"/>	
Justification	
Distribution/	
Availability Codes	
Dist	Avail and/or Special
A-1	



## LIST OF ILLUSTRATIONS

		<u>Page</u>
Figure 3.1	The initial behavior of the signal.....	44
Figure 3.2	A few cycles of the signal minus its mean.....	45
Figure 3.3	Natural log of the signal power-periodogram.....	47
Figure 3.4	Natural log of the signal spectrum.....	48
Figure 3.5	Natural log of signal spectrum plus Gaussian white noise.....	49
Figure 3.6	Natural log of signal spectrum plus Gaussian white noise with more noise power.....	50
Figure 3.7	Natural log of the squared magnitude of the signal diagonal bi-periodogram $B(f,f)$ .....	52
Figure 3.8	Natural log of the squared magnitude of the signal diagonal bispectrum.....	53
Figure 3.9	Natural log of the squared magnitude of the diagonal bispectrum of signal plus noise.....	55
Figure 3.10	Natural log of the squared magnitude of the diagonal bispectrum of signal with higher noise energy level.....	56
Figure 3.11	Natural log of the squared magnitude of the signal bi-periodogram.....	57
Figure 3.12	Natural log of the squared magnitude of the signal bi-periodogram averaged over 64 realizations...	58
Figure 3.13	Natural log of squared magnitude of bispectrum...	59
Figure 3.14	Natural log of squared magnitude of bispectrum with higher noise energy.....	60
Figure 4.1	Bi-phase primarily determines the orientation of the source of the source-receiver path.....	67

## INTRODUCTION

Passive acoustics are used to detect, classify, and localize signal sources. Present practice is based primarily on spectral and cross-spectral analysis in which phase relations between signal components of differing frequency is not exploited. Bispectral analysis is an important extension of power spectral analysis which makes use of inter-frequency phase information. MacDonald has been promoting the application of bispectra in various problems (see JSR-82-601, Speech Research, by Despain, MacDonald, and Rothaus). This collection introduces the bispectrum, and other polyspectra, and summarizes three preliminary studies exploring application to passive acoustic ASW.

The first section is a primer by G. MacDonald on bispectra and higher order spectral constructs. In this section, the auto-bispectrum and cross-bispectrum are introduced and related to third order time-lagged mean products of the time series and to higher order transfer functions connecting the process under examination to a serially independent generating function. Also discussed is use of bispectra in detecting and describing nonlinearity in the process generating the time series.

In the second section, R. Davis addresses the detectability of a signal through its spectrum and its bispectrum. Surprisingly, no processing gain derives from bispectral analysis even though it makes use of waveform (inter-frequency phase relation) information. Reliable detection requires more signal energy for bispectral detection than for spectral detection unless the signal skewness is large compared with unity. The amount of averaging applied to reduce random sampling variations is proportional to the time-bandwidth product  $N$ ; as  $N$  increases, the disadvantage of bispectral analysis increases.

In the third section H. Abarbanel describes some experiments in which numerically generated signals, rich in harmonic content, were subjected to power-spectral and bispectral analysis. These show that the signal bispectrum contains more structure than the power spectrum, indicating that bispectral analysis of signals may provide very useful additional classification beyond that obtained from energy methods. Consonant with the results of Section 2, it is found that background noise obscures the signal bispectrum and that the energy signal-to-noise ratio required for useful signal identification is comparable for spectral and bispectral analysis.

In the fourth section W. Munk outlines an application in which the inter-frequency phase information in a class of signals one might expect to be produced by submarines can be used to obtain localization information. In addition to presenting this potentially practical application, this section provides insight into the origin and description of inter-frequency phase relations using bispectra and related analytic tools.

To summarize our preliminary conclusions:

- (1) It is possible that inter-frequency phase can be used to describe aspects of source-receiver geometry, and this may have real utility in short range target trailing.
- (2) The bispectrum magnitude and phase contains information about the signal not available in the power spectrum. This could provide useful classification signatures if source waveform is not strongly dependent on geometry and operating conditions.
- (3) Bispectra do not appear to offer any advantage in detectability at low signal-to-noise ratio unless the signal skewness is large.

From a broader perspective, bispectral analysis is just one analytic tool which describes inter-frequency phase relations or waveform. These should, in general, provide additional signal description and some discrimination of signal and noise. To assess this possibility, it is necessary to understand what waveform signatures exist in real signals, how well these survive propagation, and how they may best be analyzed. Toward this end we recommend:

- (1) Submarine and surface ship signals should be analyzed for bispectral, and other waveform-descriptive, signatures. Sonobouy records obtained at high signal-to-noise ratio would be best for this purpose.
- (2) Analysis of inter-frequency phase distortion during propagation should be explored analytically to provide order-of-magnitude estimates.

Beyond passive acoustics, we hypothesize that bispectral analysis, or some other analysis tool based on inter-frequency phase relations may be useful in active acoustics in the presence of reverberation. Assuming that the target is relatively localized compared with the reflectors producing reverberation, it is likely that phase information may help discriminate target and clutter.

Some analysis is needed to quantify the gain which might be achieved.

1.0 A PRIMER ON HIGHER-ORDER OR POLYSPECTRA

Analysis of time series is the central problem of data analysis in a wide variety of defense- and intelligence-related applications. Development of the theory of time series analysis has followed two paths, communications engineering and mathematical statistics. The engineering community has emphasized the frequency or spectral approach, while the statisticians have found comfort in the time domain. Both groups have based their work on stationary linear models. These models have had great success in a wide variety of unrelated fields, and quite naturally there has been little effort to explore non-linear, non-stationary models. The very great achievements and the refined methods used in stationary linear models suggest that it is unlikely that further progress in time series analysis is likely by pursuing concepts in areas such as linear predictive coding. Further, simple observations of the world around us show that actual phenomena are non-linear and non-stationary. Progress in data processing is likely to be in the direction of models which incorporate non-stationarity and non-linearity. This primer is concerned only with non-linearity. Non-stationarity will be dealt with in a separate paper.

1.1 Linear and Non-Linear Models

Any discrete stationary process  $x_t$  with a spectral density can be represented as a linear combination of an uncorrelated stationary process  $\epsilon_t$  in the form

$$x_t = \sum_{n=-\infty}^{\infty} h_n \epsilon_{t-n} \quad (1.1)$$

Equation (1.1) provides a general representation of a linear process and can easily be transformed into the familiar ARMA (autoregressive moving average model) if the function

$$g(z) = \sum_{n=-\infty}^{\infty} h_n z^n \quad (1.2)$$

can be approximated by a rational function  $\alpha(z)/\beta(z)$ . Provided that (1.2) holds, and assuming  $\beta(z)$  has constant term one, then

$$x_t + \beta_1 x_{t-1} + \dots = \alpha_0 \epsilon_t + \alpha_1 \epsilon_{t-1} + \alpha_2 \epsilon_{t-2} + \dots \quad (1.3)$$

in which  $\epsilon_t$  is an uncorrelated process

$$E[\epsilon_{t-n} \epsilon_{t-m}] = \delta_{n-m} \epsilon^2 \quad (1.4)$$

where  $\epsilon^2$  is the expected value of  $\epsilon_t^2$ .

This representation does not distinguish between uncorrelated and independent variables; a linear model is one in which

$$x_t = \sum_{n=-\infty}^{\infty} h_n e_{t-n} \quad (1.5)$$

where  $e_t$  are independent variables. Of interest is that  $\epsilon_t$ , an uncorrelated process, and  $e_t$ , an independent process, have the same second-order structure. Both have white spectra but may differ in other ways, as will be noted below. If  $\epsilon_t$  is a Gaussian process, it is both uncorrelated and independent, and the distinction between  $\epsilon_t$  and  $e_t$  vanishes;  $x_t$  is then also a Gaussian process.

In order to illustrate the difference between  $e_t$  and  $\epsilon_t$  in general, we consider the prediction problem. If the sequence  $e_t$  is strictly independent, then the past contains no information about the future, and the best predictor of  $e_t$  is its mean. This is also true for an uncorrelated process  $\epsilon_t$  provided the predictors are linear. However, the past may contain information about the future, which will be revealed if the predictors are non-linear functions of the observed values, even though the values of  $\epsilon_t$  are uncorrelated. For example, consider a process  $\eta_t$  defined by

$$\eta_t = e_t + \alpha e_{t-1} e_{t-2}$$

where, as usual,  $e_t$  represents a serially independent process with zero mean and constant variance,  $\sigma^2$ . The process  $\eta_t$  is uncorrelated and as far as its second-order properties are concerned, it behaves as an independent process. However, unlike strictly independent processes, the optimum mean square error predictor which is at most quadratic, and looks two steps back in time, is simply

$$\tilde{\eta}_{t+1} = \beta \eta_t \eta_{t-1}$$

where  $\beta = \alpha / (1 + \alpha^2 \sigma^2)^2$ .

From this simple observation, it is obvious that there are processes that do not follow the linear representation given by (1.5).

A generalization of (1.5) is

$$x_t = \sum_{i=-\infty}^{\infty} h_i e_{t-i} + \sum_i \sum_j h_{ij} e_{t-i} e_{t-j} + \sum_i \sum_j \sum_k h_{ijk} e_{t-i} e_{t-j} e_{t-k} + \dots \quad (1.6)$$

in analogy to a Taylor series expansion. Such functional expansions were first studied by Volterra and introduced into non-linear statistics by Weiner, so the expansion in (1.6) is generally known as the Volterra-Weiner expansion. One may always suppose that the coefficients  $h_{ij\dots n}$  are unaltered by permutation of the indices. Though there is a growing literature on such representations, the problem of estimating the generalized transfer functions  $h_{ij\dots n}$  has proven to be intractable primarily because of the large number of parameters involved. Progress in using such a representation is likely only if the process  $x_t$  can be represented by a small number of parameters or if the coefficients  $h_{ij\dots n}$  have some sort of "smoothness" property. In the linear case, the smoothness condition is imposed on  $H_1(f)$ , the Fourier transform of  $h_1$ , by insisting that  $H_1(f)$  be a decent function or, in the case of an ARMA process, that  $H_1(f)$  arises from a rational function.

Since transfer functions have proven to be exceedingly useful in linear problems, an obvious generalization is to define a set of generalized transfer functions by

$$H_1(f) = \sum_{\ell=-\infty}^{\infty} h_{\ell} e^{-2\pi i f \ell}$$

$$H_2(f_1, f_2) = \sum_{\ell} \sum_{m} h_{\ell m} e^{-2\pi i (f_1 \ell + f_2 m)} \quad (1.7)$$

$$H_3(f_1, f_2, f_3) = \sum_{\ell} \sum_{m} \sum_{n} h_{\ell m n} e^{-2\pi i (f_1 \ell + f_2 m + f_3 n)}$$

and so on.

If the exciting or initiating process  $e_t$  can be represented

as

$$e_t = \int_{-1/2}^{1/2} e^{2\pi i f t} dZ(f)$$

then (1.6) can be written with the defined generalized transfer functions as

$$\begin{aligned} x_t = & \int_{-1/2}^{1/2} H_1(f) e^{2\pi i f t} dZ(f) \\ & + \int_{-1/2}^{1/2} \int_{-1/2}^{1/2} H_2(f_1, f_2) e^{2\pi i (f_1 + f_2) t} dZ(f_1) dZ(f_2) \end{aligned}$$

$$\begin{aligned}
& + \int_{-1/2}^{1/2} \int_{-1/2}^{1/2} \int_{-1/2}^{1/2} H_3(f_1, f_2, f_3) e^{2\pi i(f_1 + f_2 + f_3)t} dZ(f_1) dZ(f_2) dZ(f_3) \\
& + \dots
\end{aligned} \tag{1.8}$$

In this representation,  $H_1(f)$  is the familiar linear transfer function. In the second integral,  $H_2(f_1, f_2) dZ(f_1) dZ(f_2)$  represents the contribution of the components with frequencies  $f_1$  and  $f_2$  in  $e_t$  to the frequency  $f_1 + f_2$  in  $x_t$ . In the simple case where

$$e_t = a e^{2\pi i f_0 t}$$

then

$$dZ(f) = a \delta_{f-f_0}$$

so that (1.8) gives

$$\begin{aligned}
x_t = & a H_1(f_0) e^{2\pi i f_0 t} + a^2 H_2(f_0, f_0) e^{4\pi i f_0 t} \\
& + a^3 H_3(f_0, f_0, f_0) e^{6\pi i f_0 t} + \dots
\end{aligned}$$

This is the familiar result that a non-linear process acting on a sinusoidal input at a frequency  $f_0$  produces an output containing integer multiples of the frequency  $f_0$ .

## 1.2 Polyspectra

For linear problems, the second order-moments of the excitation  $e_t$  and the process  $x_t$  are used to estimate the coefficients in an ARMA representation, though they do not completely determine the coefficients. For non-linear processes, higher-order moments and their Fourier transforms may provide an insight. For the process  $x_t$ , the third and fourth cumulants are defined by

$$\begin{aligned}
 R_3(\tau_1, \tau_2, \tau_3) &= E[(x_{t+\tau_1} - \mu_x)(x_{t+\tau_2} - \mu_x)(x_{t+\tau_3} - \mu_x)] \\
 R_4(\tau_1, \tau_2, \tau_3, \tau_4) &= E[(x_{t+\tau_1} - \mu_x)(x_{t+\tau_2} - \mu_x)(x_{t+\tau_3} - \mu_x)(x_{t+\tau_4} - \mu_x)] \\
 &\quad - E[(x_{t+\tau_1} - \mu_x)(x_{t+\tau_2} - \mu_x)] E[(x_{t+\tau_3} - \mu_x)(x_{t+\tau_4} - \mu_x)] \\
 &\quad - E[(x_{t+\tau_1} - \mu_x)(x_{t+\tau_3} - \mu_x)] E[(x_{t+\tau_2} - \mu_x)(x_{t+\tau_4} - \mu_x)] \\
 &\quad - E[(x_{t+\tau_1} - \mu_x)(x_{t+\tau_4} - \mu_x)] E[(x_{t+\tau_2} - \mu_x)(x_{t+\tau_3} - \mu_x)]
 \end{aligned}
 \tag{1.9}$$

where  $\mu_x$  is the mean of  $x_t$

$$\mu_x = E[x_t]$$

This notation, while unconventional, clearly reveals the symmetry in the  $\tau$ 's. We note that for a stationary process, the origin can be selected so that a given  $\tau$  can be set to zero, e.g.,  $R_3(\tau_1, \tau_2, 0)$  in which case (1.9) reverts to the usual form.

The third- and fourth-order polyspectra are then defined by

$$B_3(f_1, f_2, f_3) = \sum_{\tau_1=-\infty}^{\infty} \sum_{\tau_2=-\infty}^{\infty} \sum_{\tau_3=-\infty}^{\infty} R_3(\tau_1, \tau_2, \tau_3) e^{-2\pi i(f_1\tau_1 + f_2\tau_2 + f_3\tau_3)} \quad (1.10)$$

$$B_4(f_1, f_2, f_3, f_4) =$$

$$\begin{aligned} & \sum_{\tau_1=-\infty}^{\infty} \sum_{\tau_2=-\infty}^{\infty} \sum_{\tau_3=-\infty}^{\infty} \sum_{\tau_4=-\infty}^{\infty} R_4(\tau_1, \tau_2, \tau_3, \tau_4) e^{-2\pi i(f_1\tau_1 + f_2\tau_2 + f_3\tau_3 + f_4\tau_4)} \\ & - \sum_{\tau_1=-\infty}^{\infty} \sum_{\tau_2=-\infty}^{\infty} R(\tau_1, \tau_2) e^{-2\pi i(f_1\tau_1 + f_2\tau_2)} \sum_{\tau_3=-\infty}^{\infty} \sum_{\tau_4=-\infty}^{\infty} R(\tau_3, \tau_4) e^{-2\pi i(f_3\tau_3 + f_4\tau_4)} \end{aligned}$$

$$\begin{aligned}
& - \sum_{\tau_1=-\infty}^{\infty} \sum_{\tau_3=-\infty}^{\infty} R(\tau_1, \tau_3) e^{-2\pi i(f_1\tau_1 + f_3\tau_3)} \sum_{\tau_2=-\infty}^{\infty} \sum_{\tau_4=-\infty}^{\infty} R(\tau_2, \tau_4) e^{-2\pi i(f_2\tau_2 + f_4\tau_4)} \\
& - \sum_{\tau_1=-\infty}^{\infty} \sum_{\tau_4=-\infty}^{\infty} R(\tau_1, \tau_4) e^{-2\pi i(f_1\tau_1 + f_4\tau_4)} \sum_{\tau_2=-\infty}^{\infty} \sum_{\tau_3=-\infty}^{\infty} R(\tau_2, \tau_3) e^{-2\pi i(f_2\tau_2 + f_3\tau_3)}
\end{aligned}$$

The inverse transforms are then

$$R_3(\tau_1, \tau_2, \tau_3) = \int_{-1/2}^{1/2} \int_{-1/2}^{1/2} \int_{-1/2}^{1/2} B_3(f_1, f_2, f_3) e^{2\pi i(f_1\tau_1 + f_2\tau_2 + f_3\tau_3)} df_1 df_2 df_3 \quad (1.11)$$

and similarly for  $R_4(\tau_1, \tau_2, \tau_3, \tau_4)$ .

The relationships among the frequencies in  $B_3$  and  $B_4$  follow from the definition of  $R_3$  and  $R_4$ . For the representation

$$x_t - u_x = \int_{-1/2}^{1/2} e^{2\pi i f t} dZ_x(f)$$

then  $R_3$  becomes

$$\begin{aligned}
R_3(\tau_1, \tau_2, \tau_3) &= \int_{-1/2}^{1/2} \int_{-1/2}^{1/2} \int_{-1/2}^{1/2} e^{2\pi i [f_1(t+\tau_1) + f_2(t+\tau_2) + f_3(t+\tau_3)]} \\
&\cdot E[dZ_x(f_1) dZ_x(f_2) dZ_x(f_3)] \quad (1.12)
\end{aligned}$$

and similarly for  $B_4$ . For the case of a strictly stationary process, where  $B_3$  unchanged by the same shift of  $\tau_1$ ,  $\tau_2$ , and  $\tau_3$ ,  $E[dZ_x(f_1)dZ_x(f_2)dZ_x(f_3)]$  must vanish except along the plane

$$f_1 + f_2 + f_3 = 0 .$$

Then (1.11) shows that for a stationary process,

$$B_3(f_1, f_2, f_3)df_1df_2df_3 = E[dZ_x(f_1)dZ_x(f_2)dZ(f_3)] , \quad (1.13)$$

A relationship which must be interpreted with some care, since

$B_3(f_1, f_2, f_3)df_1df_2df_3$  is a singular measure, vanishing off the plane  $f_1 + f_2 + f_3 = 0$ .

In the literature, it is conventional to suppress dependence of  $B_3$  on  $f_3 = -f_1 - f_2$  so that  $B_3$  is denoted

$$B_3(f_1, f_2, f_3) = B(f_1, f_2) \quad (1.14)$$

Similarly, noting that  $f_4 = -f_1 - f_2 - f_3$ , it is customary to write

$$B_4(f_1, f_2, f_3, f_4) = B_4(f_1, f_2, f_3) \quad (1.15)$$

For historical reasons,  $B$  is known as the bispectrum and  $B_4$  the trispectrum even though (1.13) suggest that  $B$  should really be called the trispectrum and so on; we will abide by present convention.

### 1.3 Polyspectra for Gaussian Processes

A well-known result of statistical theory is that all joint cumulants higher than the second order vanish for a multivariate normal process. The immediate and important consequence is that all spectra of order higher than two vanish for a Gaussian process. The higher-order spectra would thus appear to be of use in investigating properties of a non-Gaussian stochastic process or of a non-linear system driven by a random input. As noted above, polyspectra give a measure of the phase correlation between components whose frequencies sum to zero.

While the above paragraph captures the essential features of polyspectra, there have been few genuine applications. In part, this has arisen from the large data volumes and heavy computation required to numerically evaluate higher-order spectra and in part from statistical difficulties in interpreting the results. However, it would appear that the most important impediment has been the lack of a physically understandable interpretation of polyspectra. As a first step, we consider cross polyspectrum.

#### 1.4 Cross Polyspectrum

The cross-bispectrum is a simple generalization of the bispectrum. A form of the third-order moment for two processes  $y_t$  and  $x_t$ , where for tutorial purposes  $x_t$  can be thought of as an input into a system and  $y_t$  the output, is

$$R_{\text{xyy}}(\tau_1, \tau_2, \tau_3) = E[(x_{t+\tau_1} - \mu_x)(x_{t+\tau_2} - \mu_x)(y_{t+\tau_3} - \mu_y)]$$

and the corresponding bispectrum is

$$B_{\text{xyy}}(f_1, f_2, f_3) = \int_{\tau_1=-\infty}^{\infty} \int_{\tau_2=-\infty}^{\infty} \int_{\tau_3=-\infty}^{\infty} R_{\text{xyy}}(\tau_1, \tau_2, \tau_3) e^{-2\pi i(f_1\tau_1 + f_2\tau_2 + f_3\tau_3)}$$

and if

$$y_t = \int_{-1/2}^{1/2} e^{2\pi i f t} dZ_y(f)$$

then

$$B_{\text{xyy}}(f_1, f_2, f_3) df_1 df_2 df_3 = E[dZ_x(f_1) dZ_x(f_2) dZ_y(f_3)]$$

An illustrative example of the use and limitations of the bispectral analysis is contained in the process

$$y_t = \sum_{\ell=0}^{\infty} h_{\ell} x_{t-\ell} + \sum_{\ell=0}^{\infty} \sum_{m=0}^{\infty} h_{\ell m} x_{t-\ell} x_{t-m} + N_t \quad (1.16)$$

where  $x_t$  is a zero mean stationary Gaussian process, and  $N_t$  is a zero mean noise independent of  $x_t$ . From (1.8), we see (1.16) takes the form

$$y_t = \int_{-1/2}^{1/2} H_1(f) e^{2\pi i f t} dZ_x(f) \quad (1.17)$$

$$+ \int_{-1/2}^{1/2} \int_{-1/2}^{1/2} H_2(f_1, f_2) e^{2\pi i (f_1 + f_2) t} dZ_x(f_1) dZ_x(f_2) + N_t$$

The mean of  $y_t$  is

$$E[y_t] = \int_{-1/2}^{1/2} H_2(f, -f) P(f) df \quad (1.18)$$

where  $P$  is the power spectrum

$$P(f) df = E[dZ_x(f) dZ_x(-f)]$$

The first odd-order moment of  $y_t$  is thus dependent on the quadratic transfer function  $H_2(f_1, f_2)$ .

The second-order moment  $E[y_t y_{t+\tau}]$  takes the form

$$\begin{aligned}
 R_{yy}(\tau) &= E[y_t \cdot y_{t+\tau}] \\
 &= \int_{-1/2}^{1/2} \int_{-1/2}^{1/2} H_1(f_1) H_1(f_2) e^{2\pi i(f_1 t + f_2 t)} e^{2\pi i f z} E[dZ_x(f_1) dZ_x(f_2)] \\
 &\quad + \int_{-1/2}^{1/2} \int_{-1/2}^{1/2} \int_{-1/2}^{1/2} \int_{-1/2}^{1/2} H_2(f_1, f_2) H_2(f_3, f_4) e^{2\pi i(f_1 + f_2)t} \\
 &\quad \cdot e^{2\pi i(f_3 + f_4)\tau} E[dZ_x(f_1) dZ_x(f_2) dZ_x(f_3) dZ_x(f_4)]
 \end{aligned}$$

(since  $x_t$  is Gaussian,  $E[dZ_x(f_1) dZ_x(f_2) dZ_x(f_3)] = 0$ ). Using the standard decomposition theorem for even-order moments of Gaussian processes,

$$\begin{aligned}
 E[dZ_x(f_1) dZ_x(f_2) dZ_x(f_3) dZ_x(f_4)] &= \\
 &= E[dZ_x(f_1) dZ_x(f_2)] E[dZ_x(f_3) dZ_x(f_4)] \\
 &\quad + E[dZ_x(f_1) dZ_x(f_3)] E[dZ_x(f_2) dZ_x(f_4)] \\
 &\quad + E[dZ_x(f_1) dZ_x(f_4)] E[dZ_x(f_2) dZ_x(f_3)]
 \end{aligned}$$

and (1.17) reduces to

$$\begin{aligned}
 R_{yy}(\tau) &= \int_{-1/2}^{1/2} H_1(f)H_1(-f) e^{2\pi if\tau} P(f)df \\
 &+ \int_{-1/2}^{1/2} \int_{-1/2}^{1/2} H_2(f_1, -f_1)H_2(f_3, -f_3)P(f_1)P(f_3)df_1df_3 \\
 &+ \int_{-1/2}^{1/2} \int_{-1/2}^{1/2} H_2(f_1, f_2)H_2(-f_1, -f_2) e^{-2\pi i(f_1\tau+f_2\tau)} P(f_1)P(f_2)df_1df_2 \\
 &+ \int_{-1/2}^{1/2} \int_{-1/2}^{1/2} H_2(f_1, f_2)H_2(-f_2, -f_1) e^{-2\pi i(f_1\tau+f_2\tau)} P(f_1)P(f_2)df_1df_2
 \end{aligned}$$

The second-order moment of  $y_t$  thus contains products of the power spectra of  $x_t$  weighted by the quadratic transfer function.

An examination of the cross bispectra is more revealing of the underlying structure of the generating process. The cross moment is

$$\begin{aligned}
 R_{yx}(n) &= E[y_{t+n}x_t] = E\left[\sum_{\ell=0}^{\infty} h_{\ell}x_t x_{t-\ell+n} + \sum_{\ell=0}^{\infty} \sum_{m=0}^{\infty} h_{\ell m}x_{t-\ell+n}x_{t-m+n}x_t\right] \\
 &= \sum_{\ell=0}^{\infty} h_{\ell}E[x_t x_{t-\ell+n}] = \sum_{\ell=0}^{\infty} h_{\ell}R_{xx}(n-\ell)
 \end{aligned}$$

since the odd-order moments of the Gaussian process vanish. Taking the Fourier transform of both sides, we obtain

$$B_{yx}(f) = H_1(f)B_{xx}(f) = H_1(f)P(f)$$

and arrive at the familiar result for linear systems:

$$H_1(f) = B_{yx}(f)/P(f)$$

The cross-bispectrum  $B_{yxx}$  can be obtained from the representation of  $y_t$  given in (1.17):

$$E[y_t^x x_{t+l}^x x_{t+m}^x] = \int_{-1/2}^{1/2} \int_{-1/2}^{1/2} \int_{-1/2}^{1/2} e^{2\pi i [f_1 t + f_2(t+l) + f_3(t+m)]}$$

- $H_1(f) E[dZ_x(f_1) dZ_x(f_2) dZ_x(f_3)]$
- +  $\int_{-1/2}^{1/2} \int_{-1/2}^{1/2} \int_{-1/2}^{1/2} \int_{-1/2}^{1/2} e^{2\pi i [(f_1 + f_2)t + f_3(t+l) + f_4(t+m)]} H_2(f_1, f_2)$
- $E[dZ_x(f_1) dZ_x(f_2) dZ_x(f_3) dZ_x(f_4)]$

The first integral vanishes since  $x_t$  is Gaussian, and the second term can be decomposed as above so that

$$\begin{aligned}
 E[y_t x_{t+l} x_{t+m}] &= \int_{-1/2}^{1/2} \int_{-1/2}^{1/2} H_2(f_1, -f_1) P_x(f_1) P_x(f_3) e^{2\pi i f_3(l-m)} df_1 df_3 \\
 &+ \int_{-1/2}^{1/2} \int_{-1/2}^{1/2} H_2(-f_2, -f_1) P_x(f_1) P_x(f_2) e^{2\pi i(lf_1 + mf_2)} df_1 df_2 \\
 &+ \int_{-1/2}^{1/2} \int_{-1/2}^{1/2} H_2(-f_1, -f_2) P_x(f_1) P_x(f_2) e^{2\pi i(f_1 l + f_2 m)} df_1 df_2
 \end{aligned}$$

We now consider the quantity

$$\tilde{R}_{yxx}(\ell, m) = E[y_t x_{t+l} x_{t+m}] - E[x_{t+l} x_{t+m}] E[y_t]$$

From (1.18) we note that the first integral in (1.20) is just

$E[x_{t+l} x_{t+m}] E[y_t]$ , so that

$$\tilde{R}_{yxx}(\ell, m) = 2 \int_{-1/2}^{1/2} \int_{-1/2}^{1/2} H_2(-f_1, f_2) P(f_1) P(f_2) e^{2\pi i(lf_1 + mf_2)} df_1 df_2$$

Since  $h_{lm}$  can be made symmetric in  $l$  and  $m$ , then  $H_2(f_1, f_2)$  is symmetric in  $f_1$  and  $f_2$ . The cross-bispectrum  $B_{yxx}(f_1, f_2)$  is then

$$B_{yxx}(f_1, f_2) = 2H_2(-f_1, -f_2)P(f_1)P(f_2)$$

and the quadratic transfer function is determined by

$$H_2(f_1, f_2) = B_{yxx}(-f_1, -f_2)/2P(f_1)P(f_2)$$

For the particular process given in (1.17), it is possible to recover the linear and quadratic transfer functions by measuring the power spectrum of the input  $x_t$ , the cross spectrum  $B_{yx}$ , and the cross-bispectrum  $B_{yxx}(f_1, f_2)$ . For more general processes with terms of various orders, this is no longer possible, and an iterative calculation is required.

### 1.5 Meaning of a Finite Bispectrum

If a time series  $y_t$  has a statistically significant non-vanishing bispectrum, then two interpretations are possible. The generating process contains non-linearities which may be described in the form of (1.6) or possibly some other representation, with the

excitation function  $e_t$  being Gaussian or non-Gaussian. Alternatively, the generating model for the process is purely linear but the excitations  $e_t$  are non-normal, have a finite skewness, and are independent. In this case, the third-order moment for

$$x_t = \sum_{l=-\infty}^{\infty} h_t e_{t+l}$$

is

$$E[x_t x_{t+l} x_{t+m}] = E[e_t^3] \sum_t h_t h_{t+l} h_{t+m}$$

since  $e_t$  are independent. From the definition of the linear transfer function  $H_1(f)$ ,

$$H_1(f) = \sum_{t=0}^{\infty} h_t e^{i2\pi ft}$$

the bispectrum of  $x_t$  is

$$B_x(f_1, f_2) = E[e_t^3] H_1(f_1) H_1(f_2) H_1(-f_1 - f_2)$$

The power spectrum of  $x_t$  is just

$$P_x(f) = \text{const } |H_1(f)|^2$$

so that the square of the bicoherence given by

$$\frac{|B_x(f_1, f_2)|^2}{P_x(f_1) P_x(f_2) P_x(f_1 + f_2)}$$

is also a constant. Thus for a linear system with a Gaussian input, the bicoherence will vanish, and a linear system with a non-Gaussian input will have a constant bicoherence not zero, provided the input has a finite skewness.

The determination of the bispectrum does not by itself permit the identification of a non-linear underlying process or of a non-Gaussian excitation function. The excitation function could be non-Gaussian but have a vanishing skewness, and the resulting bispectra of  $x_t$  would vanish. Alternatively, a constant bispectrum does not imply a linear process. A finite and varying bispectrum is certainly suggestive of non-linearities in the generating process. It is for this reason that the bispectra analysis of speech, with strongly bispectral peaks for the vowels, suggests that speech production has important non-linear characteristics. Similarly, in underwater acoustics bispectral signatures may provide powerful methods for classifying sound sources.

## 2.0 BISPECTRAL DETECTION

### 2.1 Introduction

Present practice in acoustic detection rests on discriminating signal from noise on the basis of energy distribution in frequency and time. That is, waveform and phase structure of signals are not exploited. The existence of sequences of harmonically related lines in signal spectra suggests that, at least in the case of machinery produced sound, there may be useful phase information in signals of interest. Beyond this, it might be supposed that broadband signals produced by highly nonlinear hydrodynamics (flow noise and blade-rate signatures) are also associated with stable phase relations between signal components of differing frequencies. The question addressed here is whether such phase relations, if they exist and are not destroyed by propagation, could be used to enhance detectability of weak signals.

We consider the received record,  $R(t)$ , to be the sum of a signal,  $S(t)$ , and noise,  $U(t)$ . Over any record of length  $T$  starting at time  $\tau$  these have Fourier representations

$$[S(t); U(t)] = \sum_{\omega} [s(\omega, \tau); u(\omega, \tau)] e^{i\omega t}$$

where  $\omega$  is an integer multiple of  $\Delta\omega = 2\pi/T$  and

$$[s(\omega, \tau); u(\omega, \tau)] = \frac{1}{T} \int_{\tau}^{\tau+T} [S(t); U(t)] e^{-i\omega t} dt .$$

The received record has Fourier amplitudes

$$r(\omega, \tau) = s(\omega, \tau) + u(\omega, \tau)$$

For this discussion it will be assumed that records are prefiltered so that the power spectrum of noise is uniform, that is

$$P_u(\omega) \equiv \lim_{\Delta\omega \rightarrow 0} \langle |u(\omega, \tau)|^2 \rangle / \Delta\omega = P_u$$

where  $\langle \rangle$  denotes a long-time average over  $\tau$ . Further, it is assumed that noise is the sum of many contributions from independent sources and may be approximated as normally distributed. Neither of these idealizations is strictly accurate for oceanic acoustic noise, but they are fair approximations which do not prejudice the comparison made here.

The interest here is in learning how use of additional information about the nature of the signal,  $S(t)$ , affects detectability. For this comparison three simple detectors are considered.

## 2.2 The Three Detectors

Energy detection is based on some variant of the spectrogram

$$\tilde{P}(\omega, \tau) = \frac{|\tau(\omega, \tau)|^2}{\Delta\omega},$$

where the average received power is

$$\frac{1}{T} \int_{\tau}^{\tau+T} R^2(t) dt = \sum_{\omega} \Delta\omega \tilde{P}(\omega, \tau)$$

The spectrum is the time average  $P(\omega) = \langle \tilde{P}(\omega, \tau) \rangle$ . The simplest energy detector is of the form

$$D_E(\tau) = \sum_{\omega}^{\Omega} \Delta\omega \tilde{P}(\omega, \tau) - \frac{N}{N_u} \sum_{\omega}^{\Omega_u} \Delta\omega \tilde{P}(\omega, \tau) \quad (2.1E)$$

where the sums are over particular frequency regions  $\Omega$  and  $\Omega_u$ . Here  $\Omega$  is a region of positive frequencies occupied by the signal and  $\Omega_u$  is a non-overlapping region in which signal is absent.  $N$  and  $N_u$  are the number of fundamental frequency intervals in the respective frequency regions;  $N$  is the time-bandwidth product  $\Sigma \Delta\omega \cdot T/2\pi$ . The frequency regions need not be continuous and  $\Omega$  might, for example, be a series of bands encompassing various

anticipated machinery signal lines. The second term in (2.1E) simply serves to subtract from  $D_E$  an estimate of the noise contribution in the first term. In considering detector output variability, it is assumed that  $N_u \gg N$ .

Bispectral detection might be based on the bi-spectrogram

$$\tilde{B}(\omega_1, \omega_2, \tau) = \frac{r(\omega_1, \tau) r(\omega_2, \tau) r(-\omega_1 - \omega_2, \tau)}{(\Delta\omega)^2}$$

where the received signal's average cube is

$$\frac{1}{T} \int_{\tau}^{\tau+T} R^3(t) dt = \sum_{\omega_1} \Delta\omega \sum_{\omega_2} \Delta\omega \tilde{B}(\omega_1, \omega_2, \tau) .$$

The bispectrum is the time average

$$B(\omega_1, \omega_2) = \langle \tilde{B}(\omega_1, \omega_2, \tau) \rangle = |B(\omega_1, \omega_2)| e^{i\phi(\omega_1, \omega_2)},$$

where  $\phi$  is the bi-phase. From the view of signal-noise discrimination, the bispectrum is a simple construct which makes use of the phase differences between different frequencies; the particular phase information preserved is that which contributes to skewness,  $\langle R^3 \rangle$ .

A simple bispectral detector is

$$D_B(\tau) = \sum_{\omega_1}^{\Omega} \sum_{\omega_2}^{\Omega} (\Delta\omega)^2 \tilde{B}(\omega_1, \omega_2, \tau) e^{-j\hat{\phi}(\omega_1, \omega_2)} \quad (2.1B)$$

where  $\hat{\phi}$  is an a priori estimate of the bi-phase  $\phi$ . Note that since  $\tilde{B}(\omega_1, \omega_2)$  includes the Fourier amplitude at frequency  $\omega_1 + \omega_2$ , this detector makes use of energy outside  $\Omega$ . Use of this detector requires that the bi-phase be somewhat predictable so that the various terms in the sum (1B) can be phased to interfere constructively. In practice, detection could be based on  $|D_B|$ , in which case the only requirement would be that  $\phi(\omega_1, \omega_2)$  be reasonably constant for  $\omega_1$  and  $\omega_2$  in  $\Omega$ .

Maximal signal waveform information utilization is embodied in a detector based on matched filtering with a perfect replicate of the signal. Such a detector can be expressed as a convolution of signal and the record and is equivalent to

$$D_M(\tau) = \sum_{\omega}^{\Omega} s(\omega, \tau) r(-\omega, \tau) \quad (2.1M)$$

This is not, of course, a realizable detection option, since  $S$  is not known; it is included here only for comparison purposes to show what could be achieved if all signal waveform information could be used.

The three detectors have common features. All involve a sample of information from a region of frequency space  $\Omega$  and time  $T$ ; if  $\Delta\Omega$  is the bandwidth of  $\Omega$ , the size of this sample is the time-bandwidth product  $N = \Delta\Omega \cdot T/2\pi$ . If applied to a record consisting of only noise, all detectors will produce some output  $D'(\tau)$  but the average output over many realizations,  $\langle D'(\tau) \rangle$ , will vanish. In the case of energy detection,  $\langle D'_E \rangle = 0$  because a priori information about the noise spectrum was used to make  $\langle D'_E \rangle = N P_u - \frac{N}{N_u} N_u P_u = 0$ ; in practice this may not be strictly achievable but the bias,  $\langle D'_E \rangle$ , will be small.

$\langle D'_B \rangle = 0$  because the bispectrum of normally distributed noise, having no stable inter-frequency phase relations, vanishes; in reality the bias may not strictly vanish for some noise sources but it should be small unless the noise arises from a localized source which we here consider a signal.  $\langle D'_M \rangle = 0$  because noise is not correlated with signal.

### 2.3 Simplified Performance Measures

Detector sensitivity to signal may be characterized by the mean output,  $\langle D \rangle$ . For comparison purposes, the value of this mean output is

$$\langle D_E \rangle = E \quad (2.2E)$$

$$\langle D_B \rangle = qE^{3/2} \quad (2.2B)$$

$$\langle D_M \rangle = E \quad (2.2M)$$

where  $E = \langle S^2 \rangle$  is the signal variance.

The bispectral detector's signal output depends on

$$q = \frac{\int_{\omega_1}^{\Omega} \int_{\omega_2}^{\Omega} \langle s(\omega_1) s(\omega_2) s^*(\omega_1 + \omega_2) \rangle e^{-i\phi(\omega_1, \omega_2)} d\omega_1 d\omega_2}{\left[ \int_{\omega} \langle |s(\omega)|^2 \rangle d\omega \right]^{3/2}}$$

In the simplest case when the bi-phase  $\phi$  and its estimate  $\hat{\phi}$  both vanish,  $q$  is simply the signal skewness  $\langle S^3 \rangle / E^{3/2}$ . When the inter-frequency relationship is more complex there is no simple interpretation of  $q$  but it remains true that there is no a priori bound which can be placed on its magnitude. If the probability density function of  $S$  is sufficiently dispersed (i.e. the probability of extreme values is much greater than for a Gaussian distribution with the same variance) then large values of  $q$  are possible. On the other hand, if the probability density is central (with extreme

values having probabilities comparable to a normal distribution) then  $q$  will be of order unity. Without knowledge of the signal's bi-spectral character no finer bound can be placed on  $q$ . Our approach here is aimed at the order-unity- $q$  case. We note that if the distribution of  $S$  is dispersed on  $q$  can be large, but to make use of the extreme values of  $S$  which make  $q$  large will require use of long range records, much longer than the  $T$  required to achieve frequency resolution. Further, the extreme events responsible for large  $q$  would also be large individual events to an energy detector (such as  $D_E$ ) and might be detected on this basis.

In principle, (2.2E) is valid for any  $\Omega$ ,  $T$  but in practice time varying sources or Doppler shifting would require  $\Omega$  to increase with  $T$ . Achieving (2.2B) requires that the phase of the bi-spectrogram be perfectly stable and predicted by  $\hat{\phi}$  of (2.1B). Frequency dependent propagation delays would thus degrade this output in practice and, to the extent that differential propagation delays increase with frequency separation, would place an upper limit on the bandwidth of  $\Omega$ ; similarly, time varying source structure or Doppler shifting would make prediction of variations of bi-phase more difficult as  $T$  increases. Achieving (2.2M) requires a perfect matched filter in the presence of propagation phase distortion and the requirements for this become more stringent as  $T$  or the

bandwidth of  $\Omega$  increases. In the spirit of a simple comparison we have assumed that  $T$  and  $\Omega$  are chosen such that frequency and phase stability do not degrade the detector signal outputs (2.2).

In the absence of signal the detector outputs,  $D'$ , are random variables with standard deviations,  $\sigma = \langle |D'|^2 \rangle^{1/2}$ , which can be computed under the assumption that the noise is normally distributed and stationary:

$$\sigma_E = N^{1/2} P_u \Delta\omega \quad (2.3E)$$

$$\sigma_B = \sqrt{2} N [P_u \Delta\omega]^{3/2} \quad (2.3B)$$

$$\sigma_M = E^{1/2} [P_u \Delta\omega]^{1/2} \quad (2.3M)$$

Here  $N$  is the number of (positive) fundamental frequencies in  $\Omega$ . The probability density function of each  $D'$  differs and depends on  $N$ . For  $N = 1$  (extreme narrow band processing),  $D'_E$  is distributed as  $\chi_2^2 / \langle \chi_2^2 \rangle - 1$  where  $\chi_2^2$  is a chi-squared variable with two degrees of freedom.  $D'_B$  is distributed as  $Y_1 Y_2^{1/2} \exp(i\theta)$  where  $Y_1$  and  $Y_2$  are independent  $\chi_2^2$  variables and  $\theta$  is uniformly distributed over  $[0, 2\pi]$ .  $D'_M$  is normally distributed, as are  $D'_E$  and  $D'_B$  in the limit  $N \rightarrow \infty$ .

Comparison of the different detectors is made difficult because (1)  $\langle D_B \rangle$  depends on the skewness,  $q$ , and the signal variance  $E$  whereas  $\langle D_E \rangle$  and  $\langle D_M \rangle$  depend only on  $E$ , and (2) the bispectral detector makes use of energy outside the signal bandwidth  $\Omega$  whereas the other detectors depend only on the energy within  $\Omega$ . There is no limit to the size of the skewness and the larger  $q$ , the more useful is bispectral detection.

For comparative purposes, results are presented in terms of the signal to noise ratio

$$\rho = E / \int_{\omega}^{\Omega} P_u(\omega) \Delta\omega ,$$

the ratio of signal variance,  $E$ , to the noise variance in  $\Omega$ ,  $NP_u \Delta\omega$ . In terms of  $\rho$ , the mean signal to noise ratios are

$$\langle D_E \rangle / \sigma_E = N^{1/2} \rho \quad (2.4E)$$

$$\langle D_B \rangle / \sigma_B = (N/2)^{1/2} q \rho^{3/2} \quad (2.4B)$$

$$\langle D_M \rangle / \sigma_M = N^{1/2} \rho^{1/2} \quad (2.4M)$$

## 2.4 Comparison

To compare detectabilities, we imagine the detection criteria

$$D_E > D_{EC}, \text{Real} \{D_B\} > D_{BC}, \text{Real} \{D_M\} > D_{MC},$$

where the thresholds  $D_{EC}$ ,  $D_{BC}$ ,  $D_{MC}$  are set to produce a specified probability of false alarm (PFA). The signal strength required for reliable detection at the specified PFA is then characterized by  $\rho(\text{PFA})$ , the signal-to-noise ratio required to produce signal output  $\langle D \rangle$  equal to the threshold for false alarm rate PFA.

Of fundamental interest is how the detectable signal-to-noise ratio depends on the time-bandwidth product  $N$  as  $N \rightarrow \infty$ . In this case all detectors have normally distributed outputs and

$$\rho_E(\text{PFA}) = N^{-1/2} G(\text{PFA}) \quad (2.5E)$$

$$\rho_B(\text{PFA}) = q^{-2/3} N^{-1/3} G(\text{PFA})^{2/3} \quad (2.5B)$$

$$\rho_M(\text{PFA}) = \frac{1}{2} N^{-1} G(\text{PFA})^2 \quad (2.5M)$$

where  $G(\text{PFA})$  is the value a normally distributed variable with zero mean and unit variance exceeds with probability PFA. From the dependences of  $\rho$  on  $N$  in (2.5), it is clear that the bispectral detector is inferior at large  $N$  compared with the energy detector (which makes no use of phase information in the signal) and the matched filter detector (which makes use of all information about signal waveform). The power of  $G(\text{PFA})$  appearing in (2.5) depends on which moment of the noise contributes to the detector fluctuation;  $D_M$  is essentially a first moment detector,  $D_E$  second moment, and  $D_B$  third moment. Since  $G(\text{PFA})$  is such a weak function of PFA, the power of  $G$  in (2.5) is not a significant practical consideration except at extremely small PFA.

For completeness, the extreme of narrowband processing with  $N = 1$  is associated with the following values of  $\rho$  :

PFA	$\rho_E$	$q^{2/3} \rho_B$	$\rho_M$
0.1	1.3	0.9	0.8
0.01	3.6	2.1	2.7
0.001	5.9	3.4	4.8

(2.6)

The values of  $\rho_E$  and  $\rho_M$  are determined from the  $\chi_2^2$  and normal distributions;  $\rho_B$  was found by Monte Carlo simulation using a random number generator.

It is, of course, possible to further reduce the required signal-to-noise ratio for reliable detection by incoherently averaging the energy and bispectral detectors. Use of a detector of the form

$$\hat{D}(m) = \frac{1}{M} \sum_{m=1}^M D(\tau_m)$$

reduces the standard deviations,  $\sigma$ , in (3) by a factor of  $M^{-1/2}$ . In this case, the relations (2.4) and (2.5) pertain so long as  $N$  is the total time-bandwidth product  $M\Omega/\Delta\omega$ .

## 2.5 Conclusion

The energy signal-to-noise ratio required for signal detection by spectral and bispectral detectors depends on both the detector time-bandwidth product,  $N$ , and the acceptable probability of false alarm, PFA. As  $N$  increases, bispectral detection shows a relative disadvantage of the order  $N^{1/6}$ . Its disadvantage decreases as the PFA is reduced. However, for realistic time-bandwidth

products the bispectral detection disadvantage is modest. Even for a bandwidth of 100 Hz and a coherent processing time of 2 hours, the  $N^{1/6}$  factor corresponds only to a 10 db difference in required signal-to-noise at a PFA of 0.001; one minute integration corresponds to 6 db. The signal-to-noise required for bispectral detection also depends on the signal skewness,  $q$ . If  $q$  is large enough, it can compensate for the  $N^{1/6}$  bispectral disadvantage. Bispectral detectability also depends on how well the theoretical maximum (2.2B) can be approached. The critical optimistic assumption in (2.2B) is that the bi-phase of the received signal is predictable. This requires (1) that the signal bi-phase at the source be stable, (2) that it be predictable, and (3) that inter-frequency phase relations not be significantly altered by propagation from source to receiver.

We cannot assess the degree of optimism associated with the assumption of predictable signal bi-phase. First, we have no information on the inter-frequency phase relations in real signals. It is expected that there will be stable phase relations between machinery harmonics, but if these depend on geometry (as supposed in Munk's localization concept), or on source identity (which would permit bispectral classification), they will be difficult to predict

and thus detectability will be degraded. Finally, some careful work on phase distortion is required to determine if bi-phase would remain stable when acoustic propagation is multi-path.

### 3.0 BISPECTRAL EXPERIMENTS

#### 3.1 Introduction

We are interested here in exploring (1) the bispectral signatures of signals generated by highly nonlinear, quasi-periodic processes, and (2) the efficacy of bispectral analysis in extracting such signals from noise. Toward this end, signals rich in harmonic content were generated numerically, purposely contaminated by Gaussian white noise, and subjected to spectral and bispectral analysis.

The signal  $a(k)$   $k = 1, \dots, N$  was generated by solving the coupled nonlinear differential equations

$$\frac{da}{dt} = a - y - \sin z$$

$$\frac{dy}{dt} = -y + aw + ga$$

(3.1)

$$\frac{dw}{dt} = -w - ay$$

$$\frac{dz}{dt} = a$$

in which we have one adjustable parameter:  $g$ . As  $g$  varies, so does the topological character of the solution to (3.1). For  $g < 1.5$  the solution for long times,  $t$ , is  $a = y = w - z = 0$ . For  $g > 1.5$  periodic and more complicated asymptotic motion ensues.

We solved (3.1) for a variety of  $g$  in the range  $2 < g < 4$  for the initial conditions  $a(0) = y(0) = w(0) = 1.0$  and  $z(0) = 0.5$ , which has no special significance. We then stepped the solution for, typically,  $10^4$  steps and discarded the first few thousand points to remove the influence of transients reflecting the initial conditions. In Figure 3.1 we show  $a(k) = a(k\Delta t)$ , where  $\Delta t$  is a fixed time step used in the solution of (1), at  $g = 2.5615$ . The initial transient is visible as is the final asymptotic behavior. The latter is shown again in Figure 3.2 to emphasize the non-sinusoidal nature of our signal. In Figure 3.2  $a(k)$  minus its average ( $av$ ) is displayed. All results to be shown here correspond to the choice  $g = 2.5615$  shown in Figure 3.2.

### 3.2 Power Spectrum

The power spectrum of the signal  $a(k) - av$  was generated from a series of 2048 points taken from the asymptotic orbit (Figure 3.2). A cosine taper was applied to the first fifty and last fifty

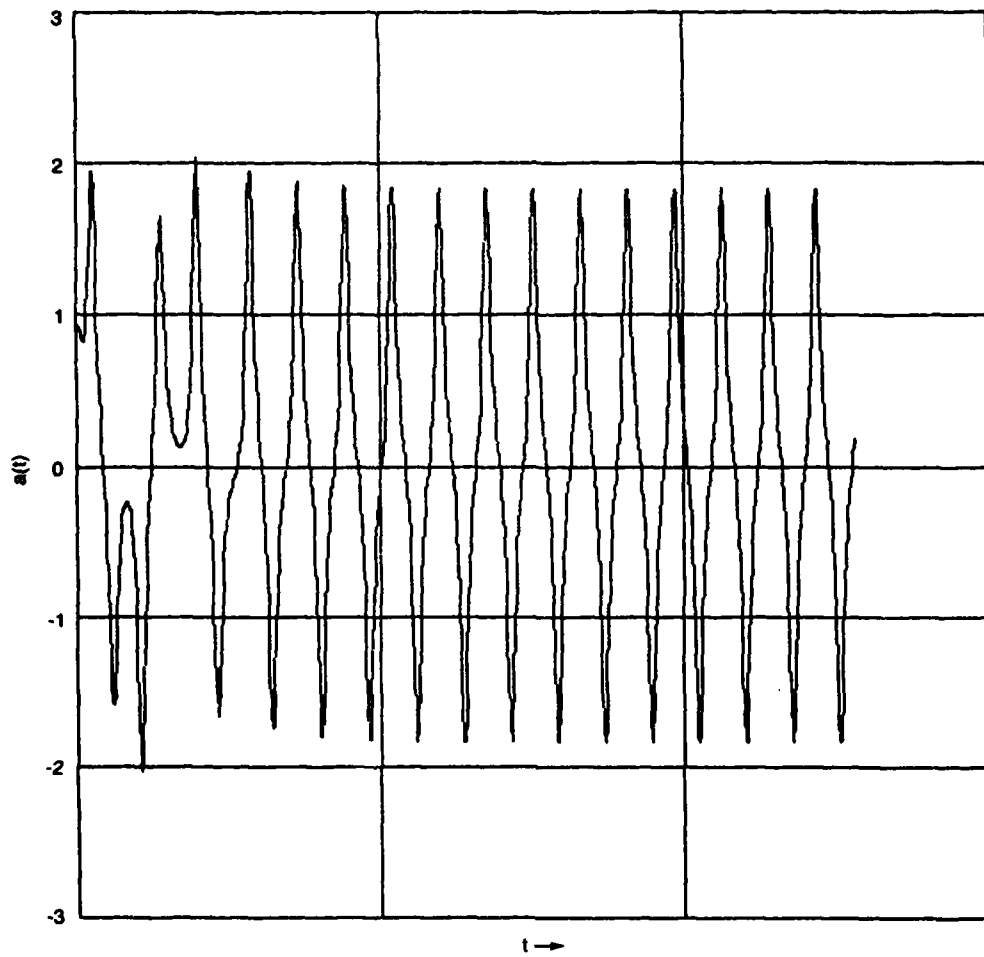


Figure 3.1 The initial behavior of the "signal" defined by (3.1) with the parameter  $g = 2.56$ .

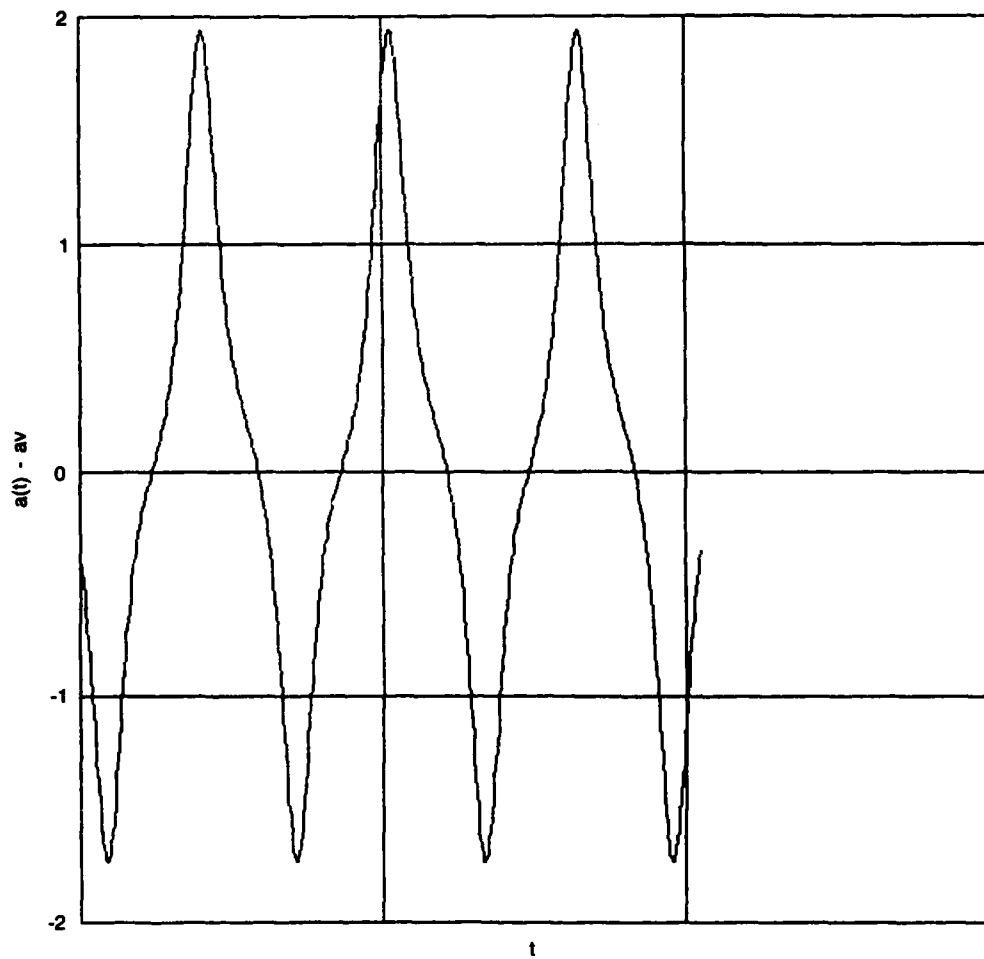
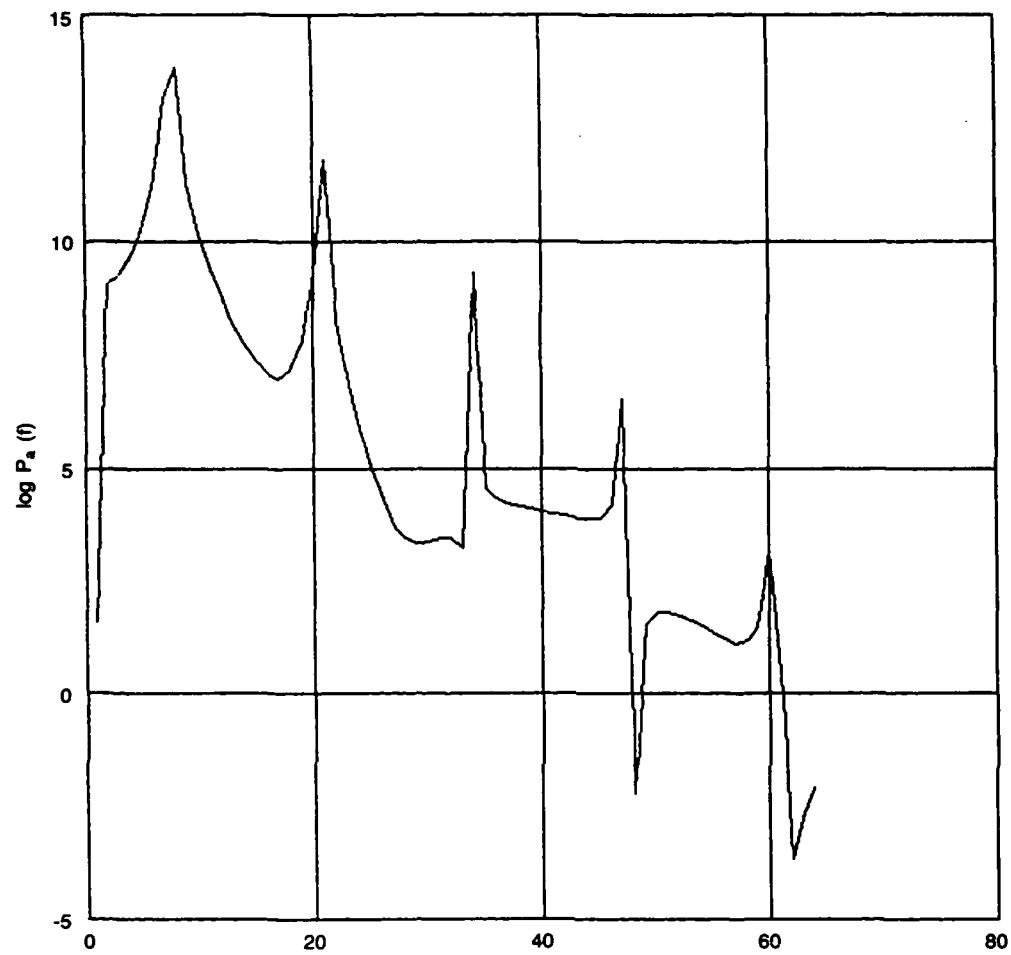


Figure 3.2 A few cycles of the signal minus its mean long after initiation.

points to smooth the discontinuities of the chopped signal. Figure 3.3 shows the natural log of the power spectrum for the first 64 frequencies of the 1024 computed. In Figure 3.4 the averaged power spectrum, generated by taking  $2^6 = 64$  samples of length  $2^{11} = 2048$  from a data sample of  $2^{17}$  points of  $a(k)$ , is presented. Each sample was tapered and Fourier transformed, then the spectrum was averaged over 64 samples. This averaging should have little effect on the signal spectrum, which is, in fact, what we see. Averaging eliminates some of the effects of noise in our samples (noise arising from machine round off errors) and of the phase relation between the signal oscillations and the record ends.

Next we added Gaussian random noise with a white spectrum to the signal and processed the noisy signal in the same fashion. In Figures 3.5 and 3.6 the power spectrum of the contaminated signal is shown for two different levels of power in the noise. In Figure 3.5 everyone would see the fundamental and sharp eyed optimists also can make out a harmonic (or two?). In Figure 3.6 even the optimists are restricted to being fundamentalists.

The problem of detecting the signal spectrum peaks in Figures 3.5 and 3.6 is, of course, an example of energy detection as discussed in Section 2. Within this context, the task is to



**Figure 3.3** Natural logarithm of the signal power-periodogram computed from a single realization. Only the lowest 64 frequencies are shown.

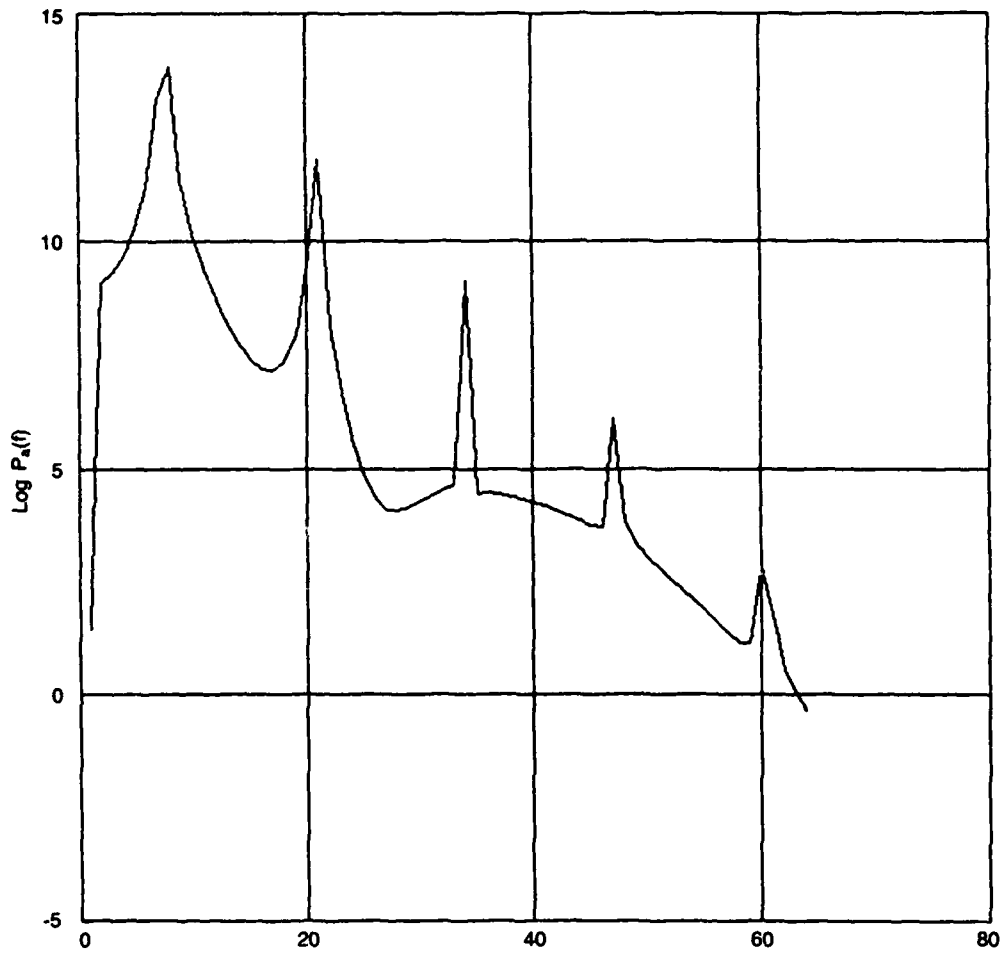
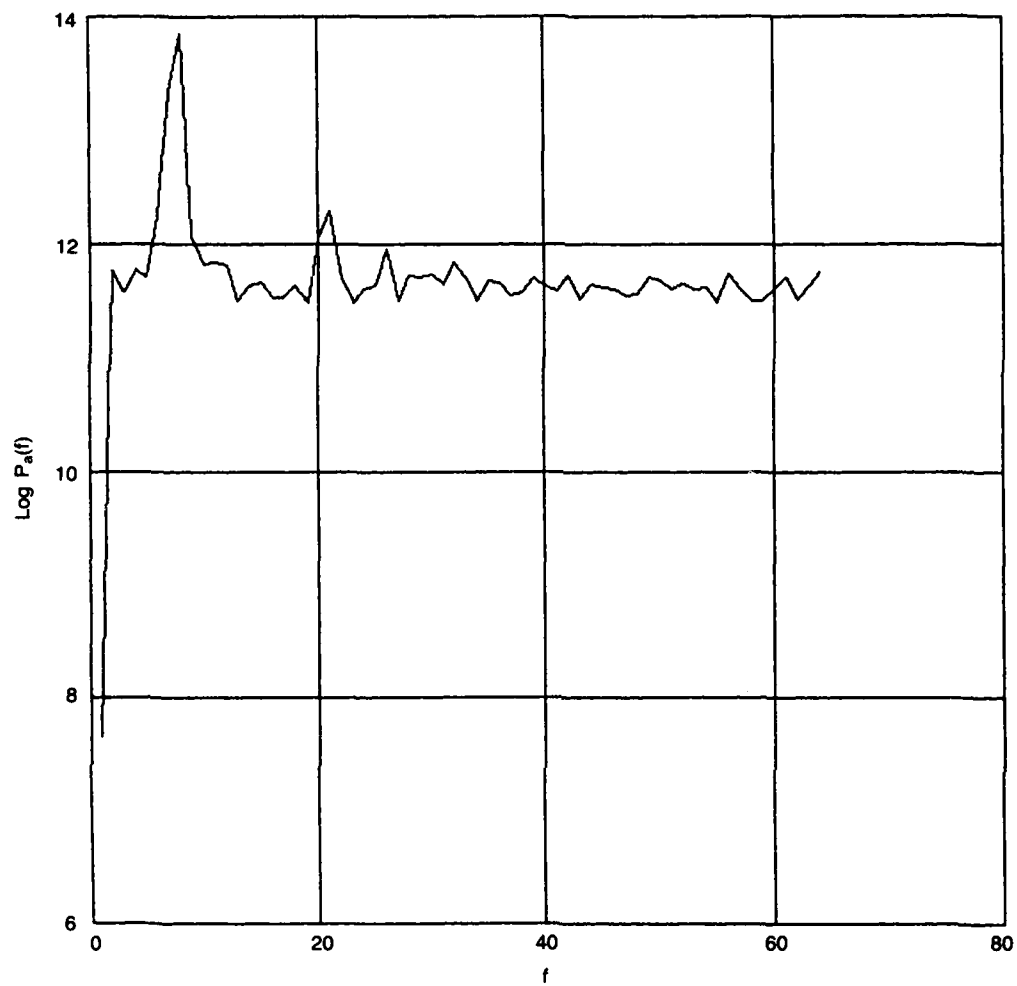


Figure 3.4 Natural logarithm of the signal spectrum computed from 64 realizations



**Figure 3.5** Natural logarithm of spectrum of signal plus Gaussian white noise computed from 64 realizations.

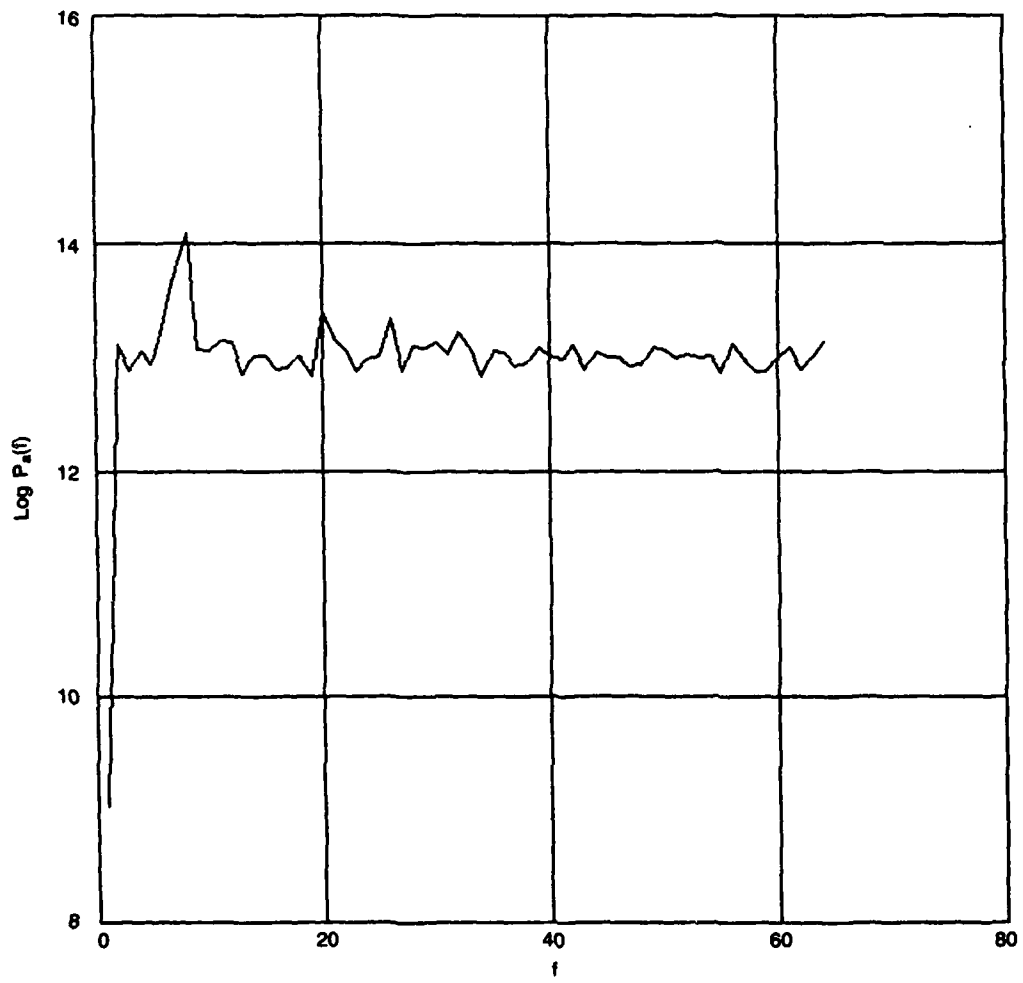


Figure 3.6 As Figure 3.5 but with more noise power

discriminate between spectral structure caused by the signal and random fluctuations of the noise spectrum. The standard deviation of the random fluctuations given by (2.3E) compares well with the evidently random wiggles in Figures 3.5 and 3.6.

### 3.3 Bispectra

Now we turn to the bispectrum. First examined was the diagonal bispectrum

$$B(f,f) = \langle \tilde{a}(f) \tilde{a}(f) \tilde{a}^*(2f) \rangle$$

where  $\tilde{a}(f)$  is the Fourier transform of  $a(k) - \bar{a}$ , with the usual cosine taper. In Figure 3.7 we display  $\log |B(f,f)|^2$  from one sample of  $2^{11}$  points; 64 frequencies are shown and there is no noise added to the signal. In Figure 3.8 we have taken 64 samples of the noise free signal and averaged  $B(f,f)$  over that ensemble. Since  $B(f,f)$  is cubic in the signal, averaging should reduce the effect of any Gaussian noise (round off error) and there is some evidence of this in Figure 3.8.

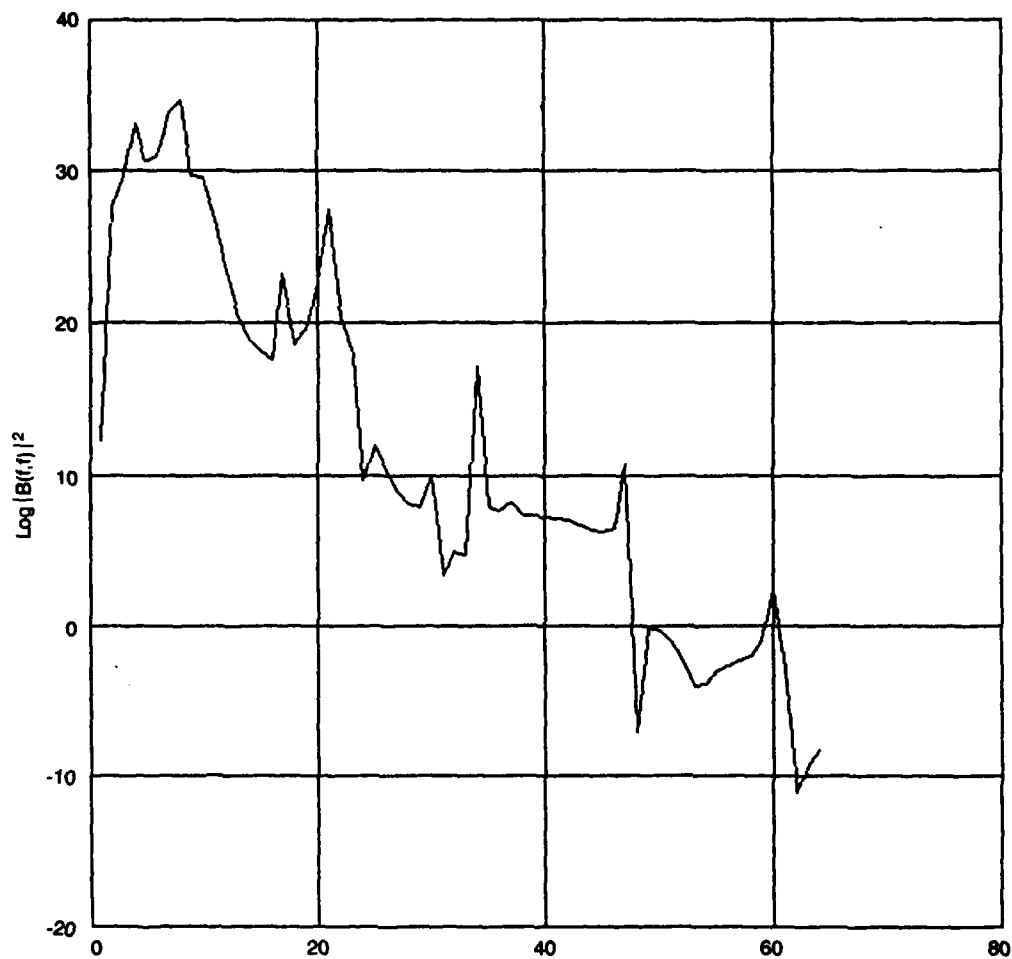


**Figure 3.7** Natural logarithm of the squared magnitude of the signal diagonal bi-periodogram  $B(f,f)$  taken from a signal realization. Only the lowest 64 frequencies are shown.

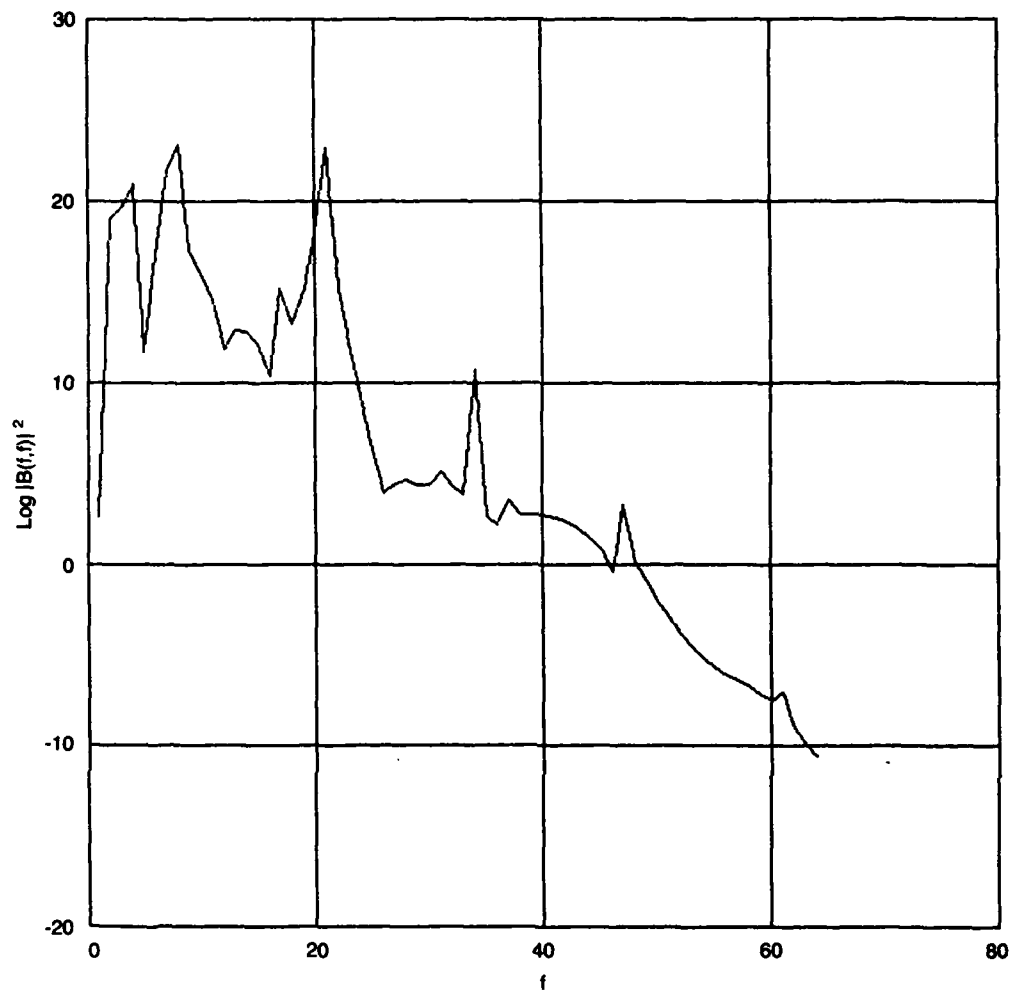


**Figure 3.8** Natural logarithm of the squared magnitude of the signal diagonal bispectrum taken from 64 realizations. Dominant peaks occur at  $f_0, 3f_0, 5f_0 \dots$  but additional structure is evident at  $1/2 f_0, 5f_0/2, 9f_0/2, 11f_0/2$ .

Figures 3.9 and 3.10 show the diagonal bispectrum of signal plus Gaussian noise for the same noise levels as used in Figures 3.5 and 3.6 for the power spectrum. It is quite clear that an ensemble of 64 members has not produced sufficient reduction of background noise to make the bispectrum a significantly more efficient signal identifier than is the power spectrum. This is consonant with the conclusions of the detectability assessment in Section 2. In fact, the bispectrum standard deviation of (2.3B) corresponds to noise levels of 31.5 and 35.5, respectively, in Figures 3.5 and 3.6. This indicates that most of the structure in these figures is due to random sampling errors.

We made one further exploration into the structure of  $B(f_1, f_2)$ . By locating the fundamental,  $f_0$ , of the signal from the power spectrum we calculated

$$B(f_0, f) = \langle \tilde{a}(f_0) \tilde{a}(f) \tilde{a}^*(f_0 + f) \rangle$$

averaged over a few frequency bins on each side of  $f_0$ . Figures 3.11 and 3.12 show  $\log |B(f_0, f)|^2$  for one sample and then averaged over 64 samples with no noise. In Figures 3.13 and 3.14 Gaussian noise was added at the previous levels and averages over 64 samples were taken.

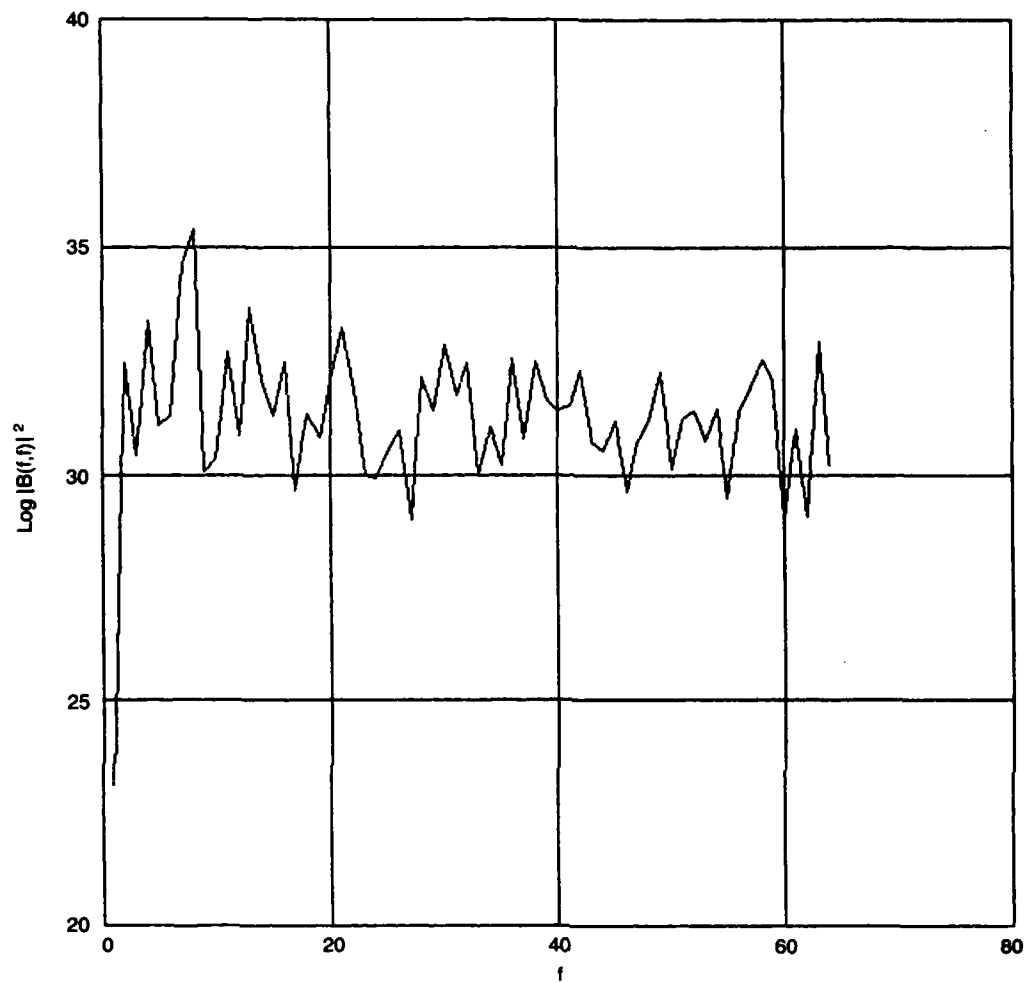


**Figure 3.9** Natural logarithm of the squared magnitude of diagonal bispectrum of signal plus noise taken from 64 realizations. The noise energy level is the same as in Figure 3.5. If enough realizations had been averaged, the noise contribution would vanish.

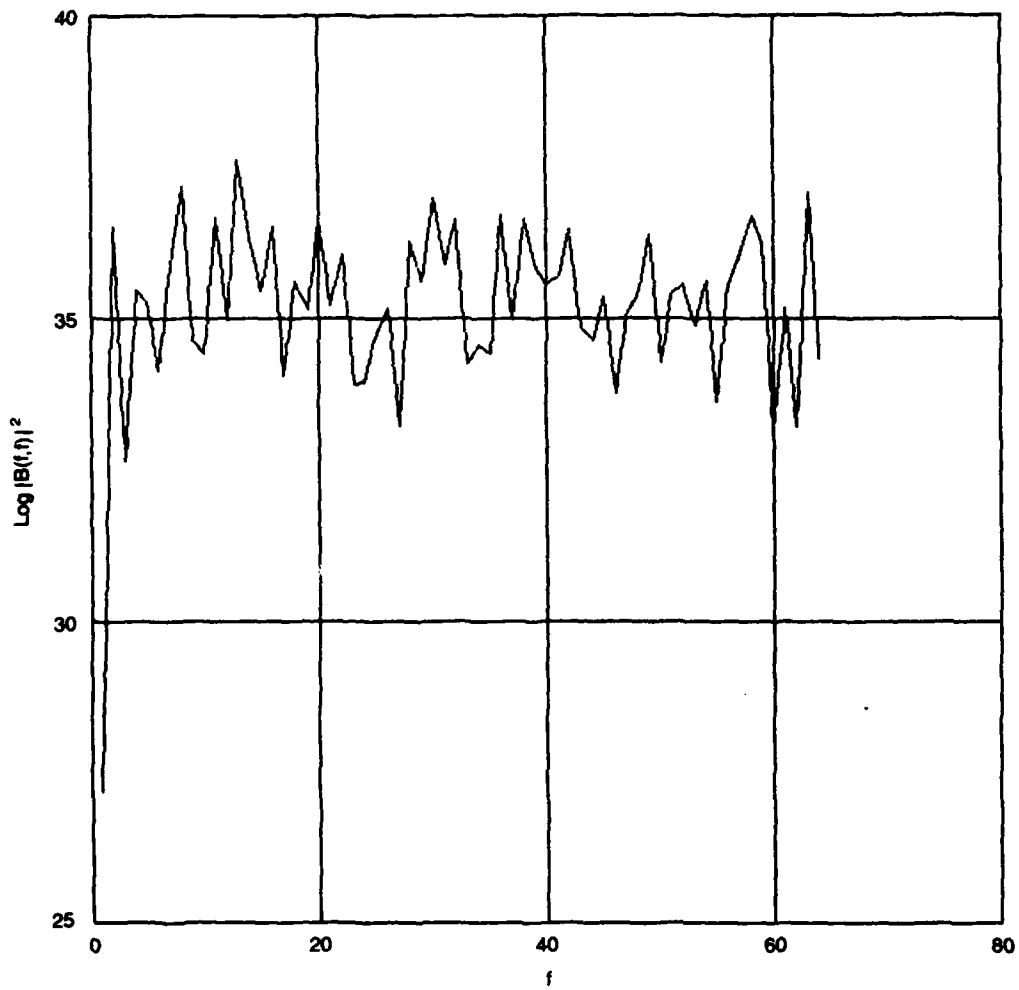
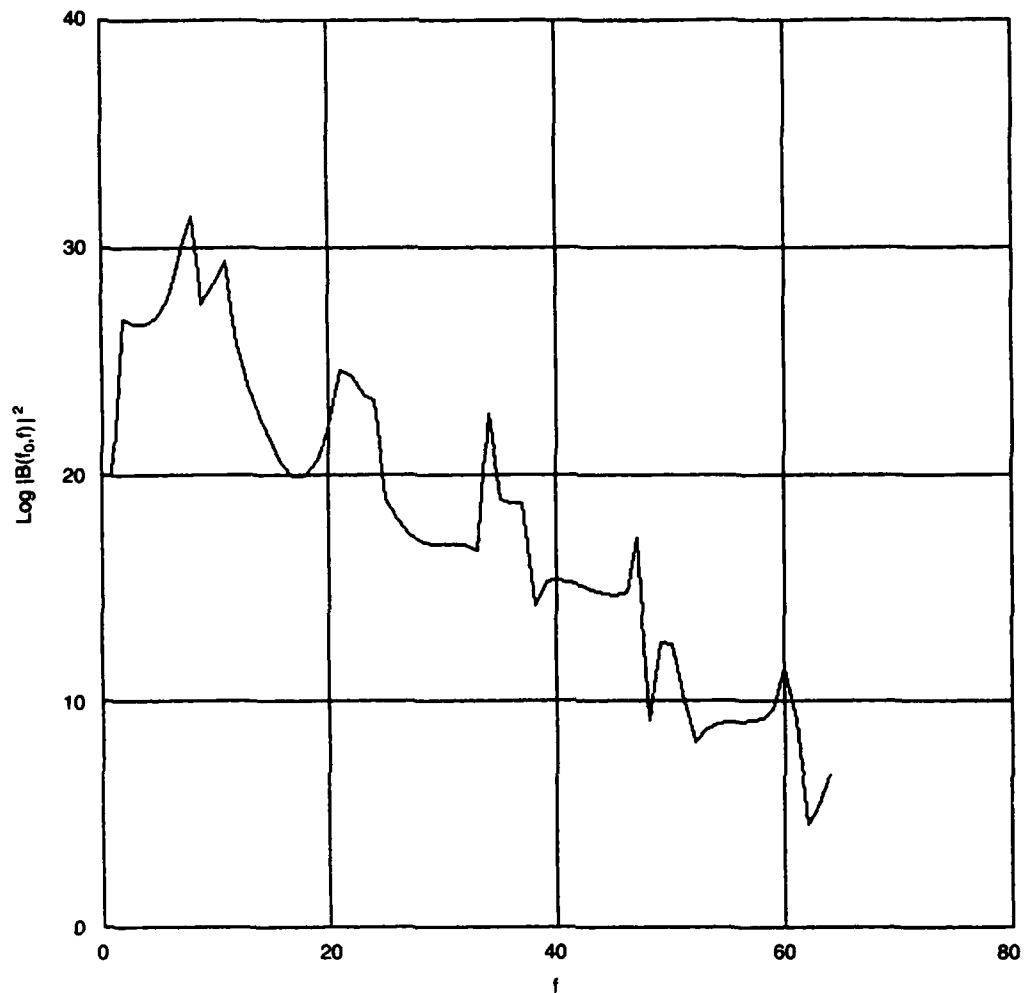


Figure 3.10 As Figure 3.9, but with the higher noise energy level used in Figure 3.6.



**Figure 3.11** Natural logarithm of the squared magnitude of the signal bi-periodogram  $B(f_0, f)$  as a function of  $f$ . The frequency  $f_0$  is the peak of the signal power spectrum (see Figure 3.4). This is an average over one realization.

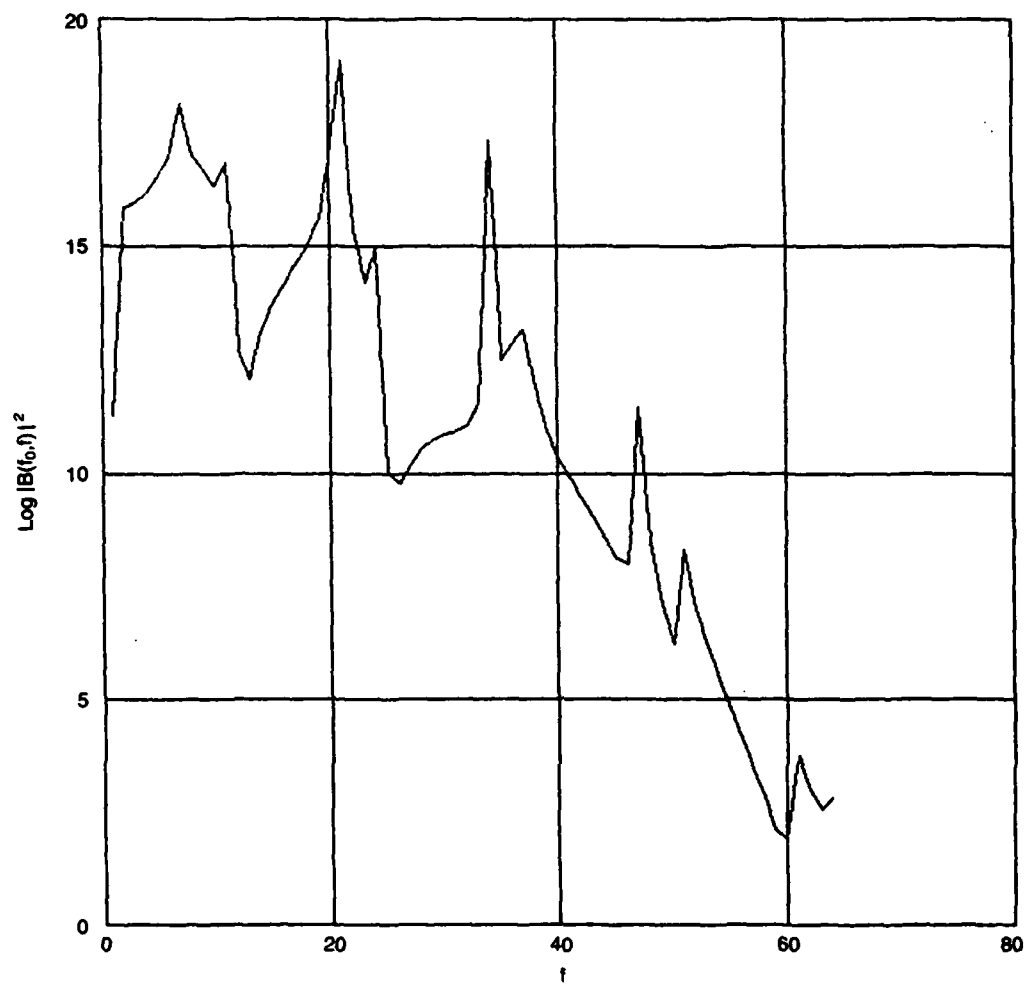
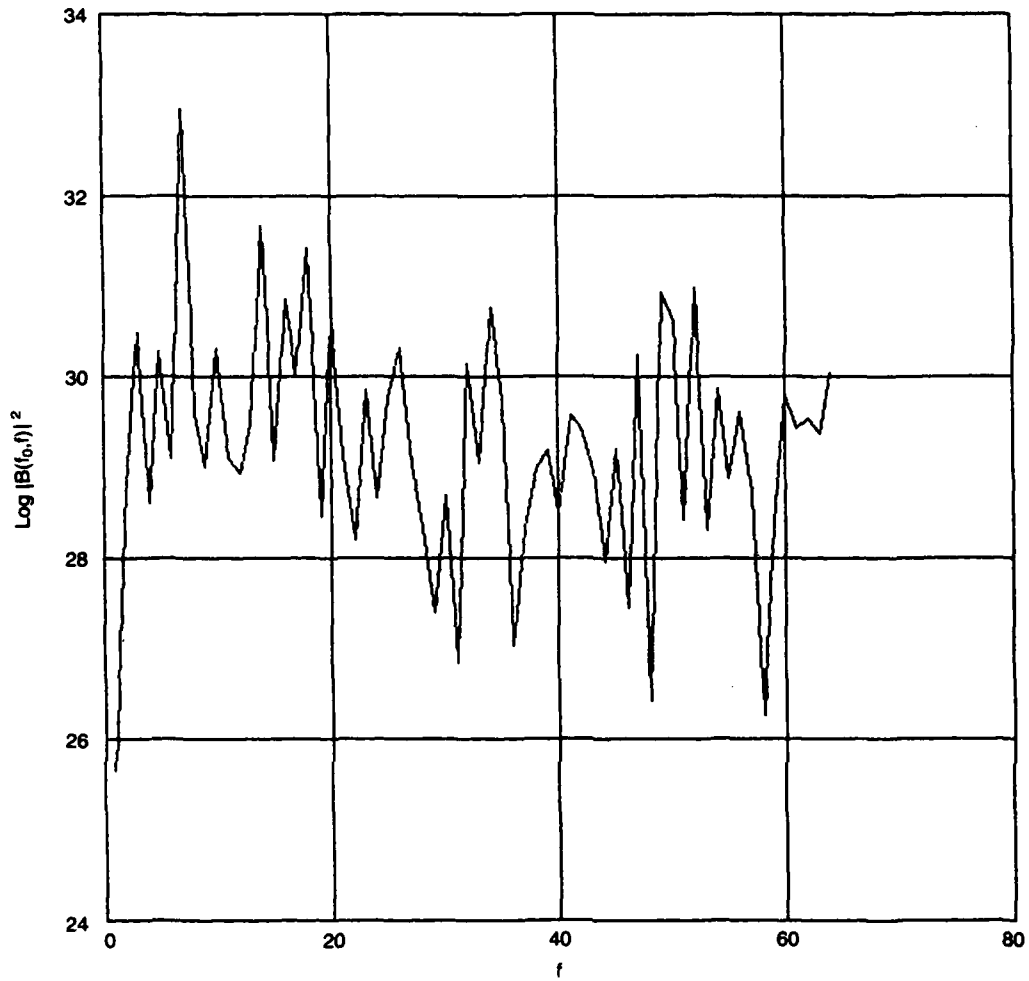


Figure 3.12 As Figure 3.1 but averaged over 64 realizations.



**Figure 3.13** Natural logarithm of squared magnitude of the bispectrum  $B(f_0, f)$  of signal plus noise obtained from 64 realizations. The noise level is the same as figures 3.5 and 3.9.

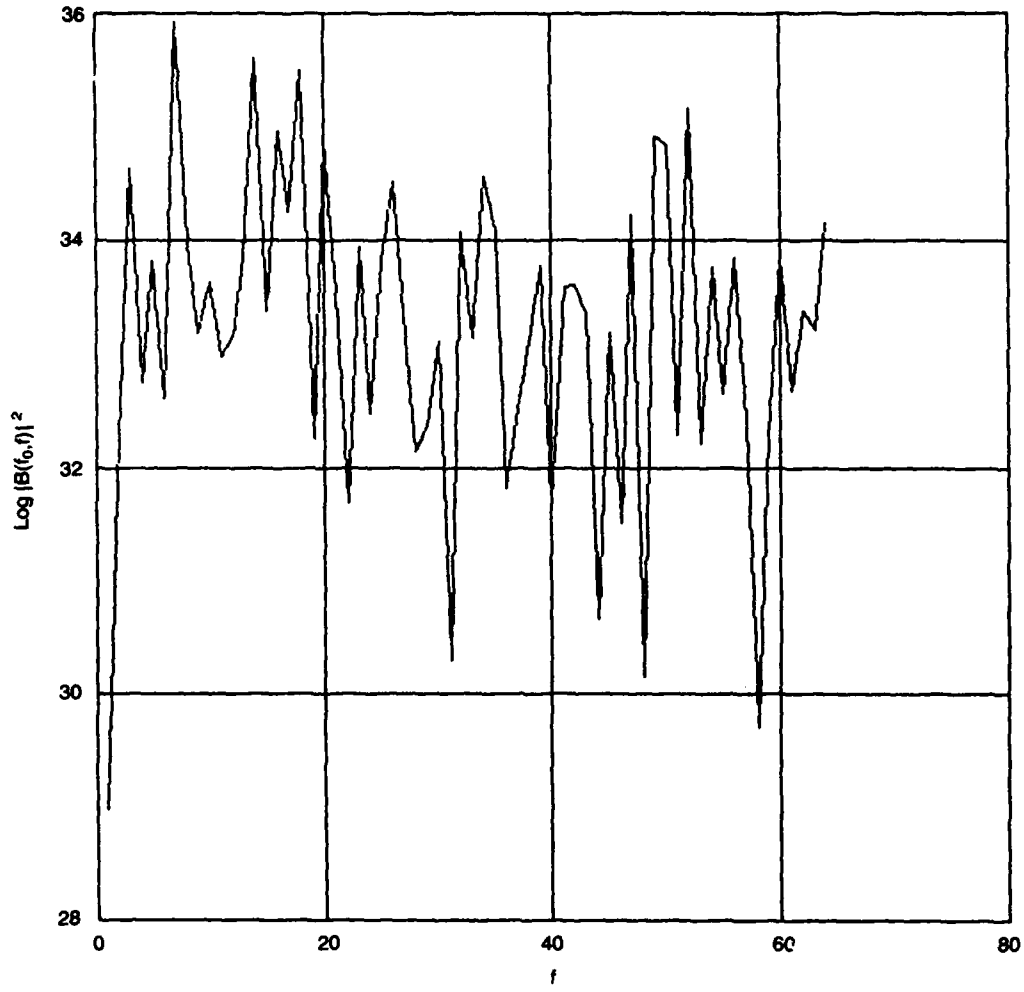


Figure 3.14 As Figure 3.13 but with the higher noise energy of figures 3.6 and 3.10.

### 3.4 Discussion

Comparison of the noise-free power spectrum (Figure 3.4), the diagonal bispectrum  $B(f,f)$  (Figure 3.8), and  $B(f_0,f)$  (Figure 3.12), provides some measure of the utility in signal classification provided by the magnitude of the bispectrum. The spectrum shows little more than a sequence of harmonic lines at  $f_0, 3f_0, \dots, (2n+1)f_0$ . The magnitude of the diagonal bispectrum, and even more so the magnitude of  $B(f_0,f)$ , shows evidence of interactions between multiples of  $f_0$  and the subharmonic  $\frac{1}{2}f_0$ . This kind of information should clearly permit discrimination of different signal sources which have identical power-spectral signatures. The phase of the bispectrum should provide even more description if it does not depend on geometry and/or source operating conditions.

All in all, the cuts of  $B(f_1,f_2)$  we have taken do not show the bispectrum to be a very valuable indicator of the presence of multiply harmonic signals in the presence of Gaussian noise.

Several caveats are, however, in order:

- (1) Our signal had weak second harmonics and subharmonics. We examined spectra and bispectra for another value of the parameter  $g$  for which strong harmonics of all orders were present. The bispectrum was rich in

detail and structure, but no signals were observed in the presence of noise using bispectra when they were not also visible in the power spectra.

- (2) We took only two cuts through the two-dimensional frequency space of the bispectrum  $B(f_1, f_2)$ . One should really display the whole 2 dimensional  $B(f_1, f_2)$  surface to exploit the value of  $B(f_1, f_2)$  without a priori bias about which cut has the essential information. The results of Kim and Powers (IEEE Trans Plasma Sci., Vol. PS-7, No. 2, June 1979, pp. 120-131) support this view. We have simply not had the time or computer expertise to explore this aspect of  $B(f_1, f_2)$ . It is not a formidable task.
- (3) Our averaging ensembles had only 64 members. Since incoherent averaging causes the standard deviation of the bispectrum to disappear only as (degrees of freedom)<sup>-1/2</sup>, we might have expected only a factor of 8 improvement at best in our averaging process. This clearly argues for bigger ensembles. We did not explore averages of the bispectrum over an area in the  $f_1, f_2$  bispectrum space. This leads to faster noise suppression but might also lead to loss of signal bispectrum unless the bi-phase changes slowly with its two frequency arguments.

## 4.0 BISPECTRAL LOCALIZATION

### 4.1 Introduction

There are many problems where phase is irrelevant. An ocean wave record taken from 10:00 to 11:00 will not differ significantly from one taken between 10:01 and 11:01. However, the phase difference between two nearby recorders gives significant information about wave direction. In order for this phase difference to be measured with adequate precision, the two recorders must be sufficiently close to give coherent records.

This is the case where cross-power-spectral analysis provides information in phase difference and coherence between two records at one frequency. In the case of auto-bispectral analysis we obtain relative phase information and bispectral coherence between two frequencies from one record. (The next step of cross-bispectral analysis between frequency  $f_1$  in record 1 and  $f_2$  in record 2 is not of interest at the moment.) We need to say what is meant by "relative phase" at two frequencies. The simplest procedure is to (i) split the record into two by pass-band filtering at  $f_1$  and  $f_2$ , (ii) heterodyne both to a single (possibly zero) frequency, and (iii) obtain the a cross spectrum between the two

records. The bispectrum provides a systematic way for doing just that. Step (iii) is, of course, in the spirit of power spectral analysis, and so some will argue that the procedure outlined is just an application of ordinary power spectra. We will take the view that any analysis involving two frequencies is distinctively different from the single frequency power spectrum analysis.

#### 4.2 The Bi-Phase

Consider two sources aboard a submarine, separated by a distance  $D$ , and emitting signals  $s'(t)$  and  $s''(t)$ , respectively. At a receiver  $R$  the received signals are

$$s'(t) = \sum_{\omega} S'(\omega) e^{i(\omega t + \psi')} , \quad \psi'(\omega) = \phi' - k(\omega)r'$$

$$s''(t) = \sum_{\omega} S''(\omega) e^{i(\omega t + \psi'')} , \quad \psi''(\omega) = \phi'' - k(\omega)r''$$

with  $k = \omega/c$  ; here  $\phi'$  and  $\phi''$  are the relative phases of the two sources and depend on  $\omega$  . For illustration, ambient noise is neglected so that the receiver hears only the sum of the two signals

$$s(t) = s' + s'' \equiv \sum S(\omega) e^{i\omega t} , \quad (4.1)$$

and it follows that

$$S(\omega) = S'(\omega) e^{i\psi'} + S''(\omega) e^{i\psi''} . \quad (4.2)$$

The bispectrum can be found as the double Fourier transform of the triple mean product of  $s$ ,

$$\text{Bi}(\omega_1, \omega_2) = \int \int d\tau_1 d\tau_2 \langle s(t) s(t-\tau_1) s(t-\tau_2) \rangle e^{i\omega_1 \tau_1} e^{i\omega_2 \tau_2} , \quad (4.3)$$

and equals

$$\text{Bi}(\omega_1, \omega_2) = |S(\omega_1)| |S(\omega_2)| |S(-\omega_1 - \omega_2)| e^{i\phi_{\text{BS}}} \quad (4.4)$$

which serves as a definition of the bispectral phase  $\phi_{\text{BS}}$  .

#### 4.3 The Simplest Case

We imagine a single frequency and its harmonic and set

$$S'(\omega) = \delta(\omega - \Omega) , \quad S''(\omega) = \delta(\omega - 2\Omega)$$

We compute  $B(\Omega, \Omega)$  from (4.3), which, on comparison with (4.4), yields

$$\phi_{BS} = 2\psi' - \psi'' = 2\phi' - \phi'' - 2k(r' - r'')$$

with  $k = \Omega/c$ .

Figure 4.1 sketches the locus of the hyperbolae which have equal range difference,  $r' - r''$ , from the sources  $s'$  and  $s''$ . These are expressed in fractions of the source separation  $D$ . For the submarine at a fixed range  $r$ , changing orientation is equivalent to moving around a circle on Figure 4.1. Suppose a trailed submarine turns on its track (which is standard operating procedure). Then  $\theta$  goes from  $0^\circ$  to  $180^\circ$ , and  $\phi_{BS}$  changes by  $4kD$ . This ought to give an early warning; the measured phase shift  $\Delta\phi_{BS}$  yields an estimate of  $D$  which is of diagnostic value. A further diagnostic is the value  $\phi_{BS} = 2\phi' - \phi''$  at mid-maneuver. The time-history of  $\phi_{BS}(t)$  for small  $r$  is slightly different than for large  $r$  which provides some information about range. Similar information might be obtained from an increase in Doppler as the target turns toward the trailer, assuming that  $\omega'$  and  $\omega''$  do not change. But the same (erroneous) conclusion would have been reached from an increase in source frequency. However, differential Doppler

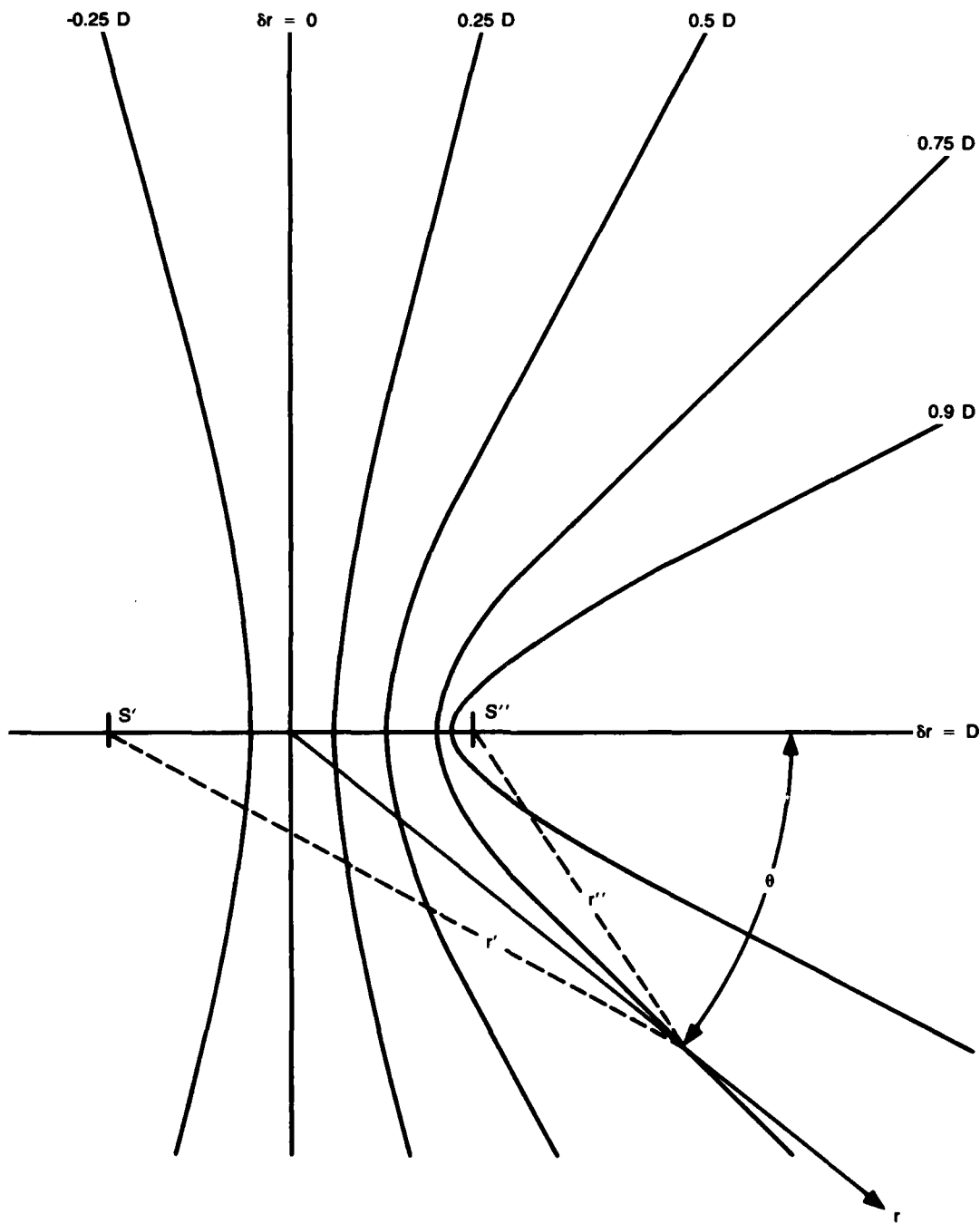


Figure 4.1  $D$  is the distance between the sources  $s'$  and  $s''$ . The differential distance  $\delta r = r' - r''$  is determined by the bi-phase. The figure shows lines of constant  $\delta r$  which are hyperbolae  $x^2/a^2 - y^2/b^2 = 1$  with  $2a = \delta r$  and  $2b = [D^2 - (\delta r)^2]^{1/2}$ . For  $r', r'' \gg D$  the asymptote  $\delta r = d \cos \theta$  obtains, showing that bi-phase primarily determines the orientation of the source of the source-receiver path

measurements on  $\omega'$  and  $\omega''$ , separately, would provide the same localization information by making use of the change in inter-frequency phase.

#### 4.4 Interpretation of Sources

The example of an  $\Omega$  generator at one point well separated from a  $2\Omega$  generator at a second point is, of course, naive. If the  $\Omega$  and  $2\Omega$  frequencies are generated at both points but with unequal intensity, then there is still this kind of information contained in  $\phi_{BS}$ , but the interpretation is more difficult.

Physically we might expect that the submarine is set into normal modes, but that the spatial distribution for  $\Omega$  modes differ from that for  $2\Omega$  modes. The interpretation is then similar, with  $D$  representing the distance between the  $\Omega$  mode centroid and the  $2\Omega$  mode centroid.

A fascinating speculation is whether similar estimations can be made from the broad-band acoustic spectrum. This is not impossible. Suppose the flow past the bow results in some resonant oscillation, and that these develop harmonics downstream associated

with hydrodynamic non-linearities. Then again we may have a situation such as the one modeled by the simple sources above.

#### 4.5 Other Frequency Ratios

One does not want to be restricted to 2:1 frequency ratios. Thus, one could go to the trispectrum for 3:1 ratios, etc., but the formalism becomes awkward. Furthermore, how would one deal with a 5:3 gear ratio?

BIBLIOGRAPHY ON THE BISPECTRUM

Akaike, H. 1966. Note on Higher Order Spectra; Annals of the Inst. of Stat. Mathe., 18:123-26.

Armstrong, J.W. 1977. Bispectral analysis of meter wavelength interplanetary scintillation; Astron. Astrophys., 61:313-320.

Aubry, M.P. 1967. Application de l'analyse bispectrale a l'etude de la diffraction, Deuxieme partie; Annales d'Astrophysique, 30:101-110.

Barnett, T.P., L.C. Johnson, P. Naitoh, N. Hicks and C. Nute. 1971. Bispectrum analysis of electroencephalogram signals during waking and sleeping; Science, 172:401-402.

Bartlett, M.S. 1967. Some remarks on the analysis of time-series; Biometrika, 54:25-38.

Borresen, R. 1978. Experimental determination of the quadratic transfer function governing slowly oscillating phenomena in irregular waves; Offshore Tech. Conf. Proc., 1:457-64.

Brillinger, D.R. 1973. An empirical investigation of the Chandler Wobble and two proposed excitation processes (Proc. of the 39th session); Bull. Int'l. Stat. Inst., 45:413-35.

Brillinger, D.R. 1973. A power spectral estimate which is insensitive to transients; Technometrics, 15:559-62.

Brillinger, D.R. 1974. An introduction to polyspectra. The London School of Economics and Political Science, 1351-74.

Brillinger, D.R. 1974. Cross-spectral analysis of processes with stationary increments including the stationary  $G/G/\infty$  queue; The Annals of Probability, 2:815-27.

Brillinger, D.R. 1974. Fourier analysis of stationary processes; Proc. IEEE, 62:1628-43.

Brillinger, D.R. 1972. On the number of solutions of systems of random equations; The Annals of Mathematical Statistics, 43:534-40.

Brillinger, D.R. 1977. The identification of a particular time series system. *Biometrika*, 64:509-15.

Brillinger, D.R. 1970. The identification of polynomial systems by means of higher order spectra. *J. Sound Vib.*, 12:301-13.

Cartwright, D.E. 1968. A unified analysis of tides and surges round North and East Britain; *Phil. Trans. Roy. Soc. London*, 263:1-55.

Chambers, J.M. 1973. Fitting nonlinear models: numerical techniques; *Biometrika*, 60:1-13.

Dalzell, J.F. 1972. Application of cross-bi-spectral analysis to ship resistance in waves; Davidson Lab, Rpt. SIT-DL-72-1606, Stevens Inst. of Tech..

Fried, D.L. 1979. Angular dependence of the atmospheric turbulence effect in speckle interferometry; *Optica Acta*, 26:597-613.

Fry, J.N. and M. Seldner. 1982. Transform analysis of the high-resolution shane-wirtanen catalog: the power spectrum and the bispectrum; *Astro. J.*, 259:474-481.

Gabrielli, C., M. Keddam and L. Raillon. 1979. Randon signals: third-order correlation measurement; *J. Phys. E: Sci. Instrum.*, 12:632-36.

Garrett, J.F. 1970. Field observations of frequency domain statistics and nonlinear effects in wind-generated ocean waves; *Inst. of Oceanography, Vancouver, B.C., Canada*.

German, V.Kh., S.P. Levikov and A.S. Tsvetsinskii. 1980. Bispectral analysis of sea-level variations; *Meteorologiya i Gidrologiya*, (Soviet Meteorology and Hydrology), 11:63-70.

Godfrey, M.D. 1965. An exploratory study of the bi-spectrum of economic time series; *Applied Statistics-J. Roy. Stat. Soc., Series C*, 14:48-69.

Hasselmann, D.E. 1978. Wind-wave generation by energy and momentum flux to forced components of a wave field; *J. Fluid Mech.*, 85:543-72.

Hasselmann, K. 1966. On nonlinear ship motions in irregular waves; *J. Ship Research*, 10:64-68.

Helland, K.N., K.S. Lii and M. Rosenblatt. 1977. Bispectra of atmospheric and wind tunnel turbulence; *Applications of Statistics*, North-Holland Publishing Company, 223-49.

Herring, J.R. 1980. Theoretical calculations of turbulent bispectra; *J. Fluid Mech.*, 97:193-204.

Hinich, M.J. 1979. Estimating the lag structure of a nonlinear time series model; *J. Am. Stati. Assoc.*, 74:449-52.

Hinich, M.J. 1981. Testing for gaussianity and linearity of a stationary time series; VA. Tech., Dept. of Economics, Blacksburg, VA.

Hinich, M.J. and C.S. Clay. 1968. The application of the discrete fourier transform in the estimation of power spectra, coherence, and bispectra of geophysical data; *Rev. Geophysics*, 6:347-363.

Huber, P.J., B. Kleiner, T. Gasser and G. Dumermuth. 1971. Statistical methods for investigating phase relations in stationary stochastic processes; *IEEE Trans. Aud. & Electroacou.*, AU-19:78-86.

Hung, G., D.R. Brillinger and L. Stark. 1979. Interpretation of kernels II. Same-signed 1st- and 2nd-degree (main diagonal) kernels of the human pupillary system; *Mathematical Biosciences*, 46:159-87.

Kedem-Kimelfeld, B. 1975. Estimating the lags of lag processes; *J. Amer. Stat. Assoc.*, 70:603-05.

Kim, Y.C., J.M. Beall, E.J. Powers and R.W. Miksad. 1980. Bispectrum and nonlinear wave coupling; *Phys. Fluids*, 23:258-63.

Kim, Y.C. and E.J. Powers. 1979. Digital bispectral analysis and its applications to nonlinear wave interactions; *IEEE Trans. Plasma Sci.*, PS-7:120-131.

Kim, Y.C. and E.J. Powers. 1978. Digital bispectral analysis of self-excited fluctuation spectra; *Phys. Fluids*, 21:1452-53.

Kim, Y.C., E.J. Powers, F. Jones and R.W. Miksad. 1981. Digital Bispectral Analysis of Nonlinear Wave Couplings in Fluids; Amer. Soc. of Mech. Eng. publ., 81-FE-32.

Lii, H-S. 1982. Model identification and estimation of nongaussian ARMA processes; Office of Naval Res., Arlington, VA, contract ONR N00014-81-K0003, Gov't. assessment ADA-120662.

Lii, K.S. and K.N. Helland. 1981. Cross-Bispectrum Computation and Variance Estimation; ACM Trans. on Mathe. Software 7:284-94.

Lii, K.S., M. Rosenblatt and C. Van Atta. 1976. Bispectral measurements in turbulence; J. Fluid Mech., 77:45-62.

Liu, P.C., and A.W. Green. 1979. Higher order wave spectra; Proc. Coastal Eng. Cong., 16th pub. ASCE, NY, 1:360-71.

Lumley, J.L. and K. Takeuchi. 1976. Application of central-limit theorems to turbulence and higher-order spectra; J. Fluid Mech., 74:433-68.

Madden, T. 1963. Spectral, cross-spectral, and bispectral analysis of low frequency electromagnetic data; Natural Electromagnetic Phenomena Below 30 KC/S Proc. NATO Advanced Study Institute, Bad Homburg, Germany, 429-50.

Mark, W.D. 1970. Spectral analysis of the convolution and filtering of non-stationary stochastic processes; J. Sound Vib., 11:19-63.

McComas, C.H. and M.G. Briscoe. 1980. Bispectra of internal waves; J. Fluid Mech., 97:205-13.

Narayanan, S. 1970. Application of volterra series to intermodulation distortion analysis of transistor feedback amplifiers; IEEE Trans. Circuit Theory, CT-17:518-27.

Ohta, M., K. Hatakeyama, S. Hiromitsu and S. Yamaguchi. 1975. Q unified study on the output probability distribution of arbitrary linear vibratory systems with arbitrary random excitation; J. Sound & Vibration, 43:693-711.

Ohta, M., S. Yamaguchi and H. Iwashige. 1977. A statistical theory for road traffic noise based on the composition of component response waves and its experimental confirmation; *J. Sound & Vibration*, 52:587-601.

Patzewitsch, J.T., M.D. Srinath and C.I. Black. 1978. Nearfield performance of passive correlation processing sonars; *J. Acoust. Soc. Am.*, 64:1412-23.

Pisarenko, V.F. 1972. On the estimation of spectra by means of non-linear functions of the covariance matrix; *Geophys. J. Roy astr. Soc.*, 28:511-31.

Ponman, T. 1981. The analysis of periodicities in irregularly sampled data; *Mon. Not. Roy astr. Soc.*, 196:583-96.

Rao, T.S. and M.M. Gabr. 1980. A test for linearity of stationary time series; *J. Time Series Analysis*, 1:145-158.

Roden, G.I. and D.J. Bendiner. 1973. Bispectra and cross-bispectra of temperature, salinity, sound velocity and density fluctuations with depth off Northeastern Japan; *J. Phys. Ocean.*, 3:308-17.

Rosenblatt, M. 1978. Energy transfer for the Burgers' equation; *Phys. Fluids*, 21:1694-97.

Rosenblatt, M. 1980. Linear processes and bispectra; *J. Appl. Prob.*, 17:265-70.

Rosenblatt, M. and J.W. Van Ness. 1965. Estimation of the bispectrum; *Annals of Math. Stats.*, 36:1120-1136.

Sasaki, K. and T. Sato. 1979. A bispectral synthesizer; *J. Acoust. Soc. Am.*, 65:732-39.

Sasaki, K., T. Sato and Y. Nakamura. 1978. An Effective Utilization of Spectral Spread in Holographic Passive Imaging Systems; *IEEE Trans. Sonics & Ultrason.*, SU-25:177-84.

Sasaki, K., T. Sato and Y. Nakamura. 1977. Holographic Passive Sonar; *IEEE Trans. Sonics & Ultrason.*, SU-24:193-200.

Sasaki, K., T. Sato and Y. Yamashita. 1975. Minimum Bias Windows for Bispectral Estimation; *J. Sound & Vibration*, 40:139-148.

Sasaki, O., T. Sato and T. Oda. 1980. Laser Doppler vibration measuring system using bispectral analysis; *Appl. Optics*, 19:151-53.

Sato, T., T. Kishimoto and K. Sasaki. 1978. Laser Doppler particle measuring system using nonsinusoidal forced vibration and bispectral analysis; *Appl. Optics*, 17:667-70.

Sato, T. and O.A. Nawa. 1968. Bispectrum analyzer using ultrasonic light deflectors; *Japan-Reports, Int'l. Congress on Acoustics*, 6:5-8.

Sato, T. and K. Sasaki. 1977. Bispectral holography; *J. Acoust. Soc. Amer.*, 62:404-07.

Sato, T., K. Sasaki and M. Taketani. 1980. Bispectral passive velocimeter of a moving noisy machine; *J. Acoust. Soc. Am.*, 68:1729-35.

Sato, T. and O. Sasaki. 1978. New 3-D laser doppler velocimeter using cross-bispectral analysis; *Applied Optics*, 17:3890-94.

Sato, T., K. Sasaki and Y. Nakamura. 1977. Real-time bispectral analysis of gear noise and its application to contactless diagnosis; *J. Acoust. Soc. Am.*, 62:382-87.

Sato, T., K. Sasaki and M. Nonaka. 1978. Prototype of bispectral passive imaging systems aiming machine-system diagnosis; *J. Acoust. Soc. Am.*, 63:1611-16.

Sato, T., K. Sasaki and N. Toyoda. 1979. A method to simulate noises from a machine system under the progress of abnormality; *J. Acoust. Soc. Am.*, 65:1331-33.

Shaman, P. 1964. *Bispectral Analysis of Stationary Time Series*, Scientific Paper 18; NY Univ, Bronx.

Tick, L.J. 1961. The estimation of "transfer functions" of quadratic systems; *Technometrics*, 3:563-67.

VanAtta, C.W. 1979. Inertial range bispectra in turbulence; *Phys. Fluids*, 22:1440-42.

Yamakawa, S. 1976. Investigation of peculiarity in some waveforms; *Bull. JSME*, 19:29-36.

Yamanouchi, Y. 1970. Application of the multiple input spectrum analysis and the higher order spectrum to the analysis of ship response in waves; Papers of the Ship Res. Insts., 33:63-103.

Yao, N-C.G and S. Neshyba. 1976. Bispectrum and Cross-Bispectrum Analysis of Wind and Currents off the Oregon Coast, I. Development; Sch. of Oceano., Oregon St. Univ, Corvallis, OR.

Yao, N-C., S. Neshyba and H. Crew. 1975. Rotary cross-bispectra and energy transfer functions between non-gaussian vector processes I. Development and example; J. Phys. Ocean., 5:164-72.

Yasui, S. 1979. Stochastic functional fourier series, volterra series, and nonlinear systems analysis; IEEE Trans. Auto. Control, AC-24:230-242.

DISTRIBUTION LIST

Dr. Marv Atkins  
Deputy Director, Science & Tech.  
Defense Nuclear Agency  
Washington, D.C. 20305

National Security Agency  
Attn RS: Dr. N. Addison Ball  
Ft. George G. Meade, MD 20755

Dr. Robert Cooper [2]  
Director, DARPA  
1400 Wilson Boulevard  
Arlington, VA 22209

Defense Technical Information [2]  
Center  
Cameron Station  
Alexandria, VA 22314

The Honorable Richard DeLauer  
Under Secretary of Defense (R&E)  
Office of the Secretary of  
Defense  
The Pentagon, Room 3E1006  
Washington, D.C. 20301

Director [2]  
National Security Agency  
Fort Meade, MD 20755  
ATTN: Mr. Richard Foss, A05

CAPT Craig E. Dorman  
Department of the Navy, OP-095T  
The Pentagon, Room 5D576  
Washington, D.C. 20350

CDR Timothy Dugan  
NFOIO Detachment, Suitland  
4301 Suitland Road  
Washington, D.C. 20390

Dr. Larry Gershwin  
NIO for Strategic Programs  
P.O. Box 1925  
Washington, D.C. 20505

Dr. S. William Gouse, W300  
Vice President and General  
Manager  
The MITRE Corporation  
1820 Dolley Madison Blvd.  
McLean, VA 22102

Dr. Edward Harper  
SSBN, Security Director  
OP-021T  
The Pentagon, Room 4D534  
Washington, D.C. 20350

Mr. R. Evan Hineman  
Deputy Director for Science  
& Technology  
P.O. Box 1925  
Washington, D.C. 20505

Mr. Ben Hunter [2]  
CIA/DDS&T  
P.O. Box 1925  
Washington, D.C. 20505

The MITRE Corporation [25]  
1820 Dolley Madison Blvd.  
McLean, VA 22102  
ATTN: JASON Library, W002

Mr. Jack Kalish  
Deputy Program Manager  
The Pentagon  
Washington, D.C. 20301

Mr. John F. Kaufmann  
Dep. Dir. for Program Analysis  
Office of Energy Research, ER-31  
Room F326  
U.S. Department of Energy  
Washington, D.C. 20545

DISTRIBUTION LIST  
(Continued)

Dr. George A. Keyworth  
Director  
Office of Science & Tech. Policy  
Old Executive Office Building  
17th & Pennsylvania, N.W.  
Washington, D.C. 20500

MAJ GEN Donald L. Lamberson  
Assistant Deputy Chief of Staff  
(RD&A) HQ USAF/RD  
Washington, D.C. 20330

Dr. Donald M. Levine, W385 [3]  
The MITRE Corporation  
1820 Dolley Madison Blvd.  
McLean, VA 22102

Mr. V. Larry Lynn  
Deputy Director, DARPA  
1400 Wilson Boulevard  
Arlington, VA 22209

Dr. Joseph Mangano [2]  
DARPA/DEO  
9th floor, Directed Energy Office  
1400 Wilson Boulevard  
Arlington, VA 22209

Mr. John McMahon  
Dep. Dir. Cen. Intelligence  
P.O. Box 1925  
Washington, D.C. 20505

Director  
National Security Agency  
Fort Meade, MD 20755  
ATTN: William Mehuron, DDR

Dr. Marvin Moss  
Technical Director  
Office of Naval Research  
800 N. Quincy Street  
Arlington, VA 22217

Dr. Julian Nall [2]  
P.O. Box 1925  
Washington, D.C. 20505

Director  
National Security Agency  
Fort Meade, MD 20755  
ATTN: Mr. Edward P. Neuburg  
DDR-FANX 3

Prof. William A. Nierenberg  
Scripps Institution of  
Oceanography  
University of California, S.D.  
La Jolla, CA 92093

Mr. C. Wayne Peale  
Office of Research and  
Development  
P.O. Box 1925  
Washington, DC 20505

The MITRE Corporation  
Records Resources  
Mail Stop W971  
McLean, VA 22102

Mr. Alan J. Roberts  
Vice President & General Manager  
Washington C<sup>3</sup> Operations  
The MITRE Corporation  
1820 Dolley Madison Boulevard  
McLean, VA 22102

Los Alamos Scientific Laboratory  
ATTN: C. Paul Robinson  
P.O. Box 1000  
Los Alamos, NM 87545

Mr. Richard Ross [2]  
P.O. Box 1925  
Washington, D.C. 20505

DISTRIBUTION LIST  
(Concluded)

Dr. Phil Selwyn  
Technical Director  
Office of Naval Technology  
800 N. Quincy Street  
Arlington, VA 22217

Mr. Leo Young  
OUSDRE (R&AT)  
The Pentagon, Room 3D1067  
Washington, D.C. 20301

Dr. Eugene Sevin [2]  
Defense Nuclear Agency  
Washington, D.C. 20305

Mr. Robert Shuckman  
P.O. Box 8618  
Ann Arbor, MI 48107

Dr. Joel A. Snow [2]  
Senior Technical Advisor  
Office of Energy Research  
U.S. DOE, M.S. E084  
Washington, D.C. 20585

Mr. Alexander J. Tachmindji  
Senior Vice President & General  
Manager  
The MITRE Corporation  
P.O. Box 208  
Bedford, MA 01730

Dr. Vigdor Teplitz  
ACDA  
320 21st Street, N.W.  
Room 4484  
Washington, D.C. 20451

Dr. Al Trivelpiece  
Director, Office of Energy  
Research, U.S. DOE  
M.S. 6E084  
Washington, D.C. 20585

Mr. James P. Wade, Jr.  
Prin. Dep. Under Secretary of  
Defense for R&E  
The Pentagon, Room 3E1014  
Washington, D.C. 20301